MPI/PhT/97–029
TTP97–18*
hep-ph/9705254
May 1997

Heavy Quark Current Correlators to $\mathcal{O}(\alpha_s^2)$†

K.G. Chetyrkin[a,b], J.H. Kühn[c] and M. Steinhauser[a]

[a] *Max-Planck-Institut für Physik, Werner-Heisenberg-Institut, D-80805 Munich, Germany*

[b] *Institute for Nuclear Research, Russian Academy of Sciences, Moscow 117312, Russia*

[c] *Institut für Theoretische Teilchenphysik, Universität Karlsruhe, D-76128 Karlsruhe, Germany.*

Abstract

In this paper the three-loop polarization functions $\Pi(q^2)$ are calculated for the cases of an external vector, axial-vector, scalar or pseudo-scalar current. Results are presented for the imaginary part which directly leads to the cross section $\sigma(e^+e^- \to Z \to \text{hadrons})$ and to the Higgs decay rates, respectively.

PACS numbers: 12.38.-t, 12.38.Bx, 13.65.+i, 13.85.Lg.

*The complete postscript file of this preprint, including figures, is available via anonymous ftp at www-ttp.physik.uni-karlsruhe.de (129.13.102.139) as /ttp97-18/ttp97-18.ps or via www at http://www-ttp.physik.uni-karlsruhe.de/cgi-bin/preprints.

†Supported by BMBF under Contract 057KA92P, DFG under Contract Ku 502/8-1 and INTAS under Contract INTAS-93-744-ext.

1 Introduction and notation

A variety of important observables are essentially given by the correlators of currents with different tensorial structure. The cross section for e^+e^- annihilation into hadrons is governed by the vector current correlator, the Z decay rate by a combination of vector and axial correlators [1]. Higgs decays can be expressed by the correlators of the corresponding scalar or pseudo-scalar current densities. Theoretical predictions for all these quantities in one- and two-loop approximation, corresponding to the Born level and the order α_s corrections, are available since long. However, in view of the present or the foreseeable experimental precision improved calculations of these quantities are required, at least up to order α_s^2, if possible even up to order α_s^3. For massless quarks the NNLO result is available both for the vector [2] and the scalar correlators [3]. Quark mass effects are often incorporated by inclusion of the lowest one or two terms in an expansion in m^2/s. This approach is well justified for many applications [1]. Even for relatively low energy values, down to about three to four times the quark mass this approach leads to an adequate result if sufficiently many terms are included in the expansion [4, 5]. Nevertheless it is desirable to calculate the correlator for arbitrary values of m^2/s without directly invoking the high momentum expansion. Recently this was achieved for both real and imaginary parts of the three-loop polarization function [6] with a heavy quark coupled to an external current. In a first step the method was applied to the case of the vector current correlator. In this paper also the axial-vector, scalar and pseudo-scalar cases are considered. This completes the relevant $\mathcal{O}(\alpha_s^2)$ corrections to polarization functions for neutral gauge bosons induced by heavy quarks, more specifically to their "non-singlet" parts. Contributions from the double-triangle diagram, giving rise to "singlet" contributions, are not considered in this work and will be treated elsewhere.

It is useful to define dimensionless variables:

$$z \;=\; \frac{q^2}{4m^2}, \qquad x \;=\; \frac{2m}{\sqrt{s}}, \tag{1}$$

where q is the external momentum of the polarization function and s is the center of mass energy in the process $e^+e^- \to$ hadrons. Then the velocity, v, of one of the produced quarks reads

$$v \;=\; \sqrt{1-x^2}. \tag{2}$$

Every time the generic index δ appears without further explanation it is understood that δ represents one of the letters a, v, s or p.

The polarization functions for the four cases of interest are defined by

$$\left(-q^2 g_{\mu\nu} + q_\mu q_\nu\right) \Pi^\delta(q^2) + q_\mu q_\nu \,\Pi_L^\delta(q^2) \;=\; i \int dx\, e^{iqx} \langle 0|T j_\mu^\delta(x) j_\nu^\delta(0)|0\rangle \;\text{ for }\; \delta = v, a\,, \tag{3}$$

$$q^2\, \Pi^\delta(q^2) \;=\; i \int dx\, e^{iqx} \langle 0|T j^\delta(x) j^\delta(0)|0\rangle \;\text{ for }\; \delta = s, p, \tag{4}$$

with the currents

$$j_\mu^v = \bar\psi \gamma_\mu \psi, \qquad j_\mu^a = \bar\psi \gamma_\mu \gamma_5 \psi, \qquad j^s = \bar\psi \psi, \qquad j^p = i \bar\psi \gamma_5 \psi. \tag{5}$$

In Eqs. (3) and (4) two powers of q are factored out in order to end up with dimensionless quantities $\Pi^\delta(q^2)$. As we are only interested in the imaginary part the overall renormalization can be performed in such a way that this is possible. Furthermore we ensure that $\Pi^\delta(0) = 0$. The transformation from this scheme to other (overall) renormalization conditions is discussed in App. A. Concerning the renormalization it should be mentioned that for the scalar and pseudo-scalar current the combinations mj^s and mj^p, where m is the pole mass, have to be considered in order to arrive at finite results. Note that $\Pi_L^v = 0$ and Π_L^a is trivially obtained from Π^p through the axial Ward identity $(q^2)^2\Pi_L^a(q^2) = 4m^2q^2\,(\Pi^p(q^2) - q^2(\partial\Pi^p(q^2)/\partial q^2)|_{q^2=0})$.

The physical observable $R(s)$ is related to $\Pi(q^2)$ by

$$R^\delta(s) = 12\pi\,\mathrm{Im}\,\Pi^\delta(q^2 = s + i\epsilon) \qquad \text{for } \delta = v, a\,, \tag{6}$$

$$R^\delta(s) = 8\pi\;\,\mathrm{Im}\,\Pi^\delta(q^2 = s + i\epsilon) \qquad \text{for } \delta = s, p\,. \tag{7}$$

It is convenient to define

$$\Pi^\delta(q^2) = \Pi^{(0),\delta}(q^2) + \frac{\alpha_s(\mu^2)}{\pi}C_F\Pi^{(1),\delta}(q^2) + \left(\frac{\alpha_s(\mu^2)}{\pi}\right)^2\Pi^{(2),\delta}(q^2) + \dots\,, \tag{8}$$

$$\Pi^{(2),\delta} = C_F^2\Pi_A^{(2),\delta} + C_AC_F\Pi_{NA}^{(2),\delta} + C_FTn_l\Pi_l^{(2),\delta} + C_FT\Pi_F^{(2),\delta} + C_FT\Pi_S^{(2),\delta}, \tag{9}$$

and similarly for $R^\delta(s)$. The abelian contribution $\Pi_A^{(2),\delta}$ is already present in (quenched) QED and $\Pi_{NA}^{(2),\delta}$ originates from the non-abelian structure specific for QCD. The polarization functions containing a second massless or massive quark loop are denoted by $\Pi_l^{(2),\delta}$ and $\Pi_F^{(2),\delta}$, respectively. $\Pi_S^{(2),\delta}$ represents the double-triangle contribution. Our procedure will be applied to the first three terms in Eq. (9), the last two terms will be studied elsewhere.

The paper is organized as follows: In the next section the expressions for the polarization functions in the different kinematical regions are provided. In Section 3 the approximation method is described and the results are given in Section 4. The conclusions are finally presented in Section 5.

2 Discussion of the kinematical regions

This section provides a discussion of three kinematical regions where analytical results are available and contains the input data required for the approximation method.

High energy region

The input from the kinematical region where $-q^2 \gg m^2$ puts stringent constraints on the form of the polarization function and plays an important rôle for our procedure. In the limit of large external momentum the polarization function can be cast into the following form:

$$\Pi^\delta(q^2) = \frac{3}{16\pi^2}\sum_{n\geq 0} D_n^\delta\frac{1}{z^n}. \tag{10}$$

The coefficients D_n^δ contain $\ln(-z)$-terms up to third order. For the subsequental discussion only the terms with $n = 0$ and 1 are needed. These first two terms can be calculated by simply Taylor expanding the diagrams in the mass [1]. This leads to massless three-loop integrals for which the technique is known since long [7]. The following decomposition of the coefficients D_n^δ is adopted:

$$\begin{aligned}
D_n^\delta &= D_n^{(0),\delta} + \frac{\alpha_s(\mu^2)}{\pi} C_F D_n^{(1),\delta} + \left(\frac{\alpha_s(\mu^2)}{\pi}\right)^2 D_n^{(2),\delta} + \dots \ , \\
D_n^{(2),\delta} &= C_F^2 D_{A,n}^{(2),\delta} + C_A C_F D_{NA,n}^{(2),\delta} + C_F T n_l D_{l,n}^{(2),\delta} + C_F T D_{F,n}^{(2),\delta}, \\
D_{x,n}^{(j),\delta} &= \sum_{k=0}^{3} d_{x,n,k}^{(j),\delta} \left(\ln\frac{-q^2}{m^2}\right)^k \qquad\qquad j \in \{0,1,2\},\ x \in \{A, NA, l, F\}, \qquad (11)
\end{aligned}$$

where $d_{x,n,k}^{(j),\delta}$ are numerical constants. For $D_n^{(0),\delta}$ and $D_n^{(1),\delta}$ the sum runs only up to $k = 1$ and $k = 2$, respectively. The results for the four cases are available in the literature [2, 8, 3]. We have independently repeated this calculation. The results in the on-shell scheme are listed in Tab. 1. Due to our renormalization condition ($\Pi^\delta(0) = 0$) for a comparison with [2, 8, 3] the terms presented in App. A have to be taken into account. The analytic expressions for D_n^v can be found in [4] and for D_n^s and D_n^p in [5]. D_0^a and D_1^a are listed in App. B.

This information will serve as input for the procedure described in Section 3. It should be noted that in contrast to the vector case treated in [6] the axial-vector, scalar and pseudo-scalar correlator also develop cubic logarithms $\ln^3(-z)$. If we had adopted the $\overline{\rm MS}$ definition for the mass and $\mu^2 = q^2$, these cubic logarithms would vanish.

Behaviour at $q^2 = 0$

An important input to the behaviour of the polarization function originates from the Taylor expansion around $q^2 = 0$. In this case the three-loop diagrams have to be expanded in the external momentum leading to massive tadpole integrals. The calculation is performed with the help of the algebraic program MATAD written in FORM [9]. It automatically expands in q up to the desired order, performs the traces and applies recurrence relations [10] to reduce the many different diagrams to a small set of master integrals. The structure of $\Pi(q^2)$ is as follows:

$$\begin{aligned}
\Pi^\delta(q^2) &= \frac{3}{16\pi^2} \sum_{n>0} C_n^\delta z^n, \\
C_n^\delta &= C_n^{(0),\delta} + \frac{\alpha_s(\mu^2)}{\pi} C_F C_n^{(1),\delta} + \left(\frac{\alpha_s(\mu^2)}{\pi}\right)^2 C_n^{(2),\delta} + \dots \ , \\
C_n^{(2),\delta} &= C_F^2 C_{A,n}^{(2),\delta} + C_A C_F C_{NA,n}^{(2),\delta} + C_F T n_l C_{l,n}^{(2),\delta} + C_F T C_{F,n}^{(2),\delta}. \qquad (12)
\end{aligned}$$

[1] Recently terms up to order $n = 4$ for the scalar and pseudo-scalar correlator [5] and up to $n = 6$ for the vector correlator [4] have been calculated. This requires also the knowledge of massive tadpole integrals.

	$n=0$				$n=1$			
k	0	1	2	3	0	1	2	3
$D_n^{(0),v}$	2.2222	-1.3333	0.0000	0.0000	2.0000	0.0000	0.0000	0.0000
$D_n^{(1),v}$	-3.9749	-1.0000	0.0000	0.0000	0.0000	-3.0000	0.0000	0.0000
$D_{A,n}^{(2),v}$	1.3075	0.1250	0.0000	0.0000	2.7727	-0.3750	2.2500	0.0000
$D_{NA,n}^{(2),v}$	-9.5651	-0.7175	0.4583	0.0000	-3.9903	-7.7083	1.3750	0.0000
$D_{l,n}^{(2),v}$	2.9723	0.2306	-0.1667	0.0000	2.2899	2.1667	-0.5000	0.0000
$D_{F,n}^{(2),v}$	-1.2583	0.2306	-0.1667	0.0000	-5.1048	2.1667	-0.5000	0.0000
$D_n^{(0),a}$	3.5556	-1.3333	0.0000	0.0000	-2.0000	2.0000	0.0000	0.0000
$D_n^{(1),a}$	-2.0860	-1.0000	0.0000	0.0000	1.9623	1.5000	-1.5000	0.0000
$D_{A,n}^{(2),a}$	-1.0387	0.1250	0.0000	0.0000	-8.7928	0.2672	-1.3125	0.7500
$D_{NA,n}^{(2),a}$	-9.8007	-0.7175	0.4583	0.0000	14.8142	-1.5224	-4.5417	0.4583
$D_{l,n}^{(2),a}$	3.6266	0.2306	-0.1667	0.0000	-8.5657	2.3606	1.3333	-0.1667
$D_{F,n}^{(2),a}$	-0.2639	0.2306	-0.1667	0.0000	6.5500	-4.5090	1.3333	-0.1667
$D_n^{(0),s}$	5.3333	-2.0000	0.0000	0.0000	-3.0000	3.0000	0.0000	0.0000
$D_n^{(1),s}$	-3.9623	-4.5000	1.5000	0.0000	7.8185	3.0000	-4.5000	0.0000
$D_{A,n}^{(2),s}$	2.0416	0.8578	3.5625	-0.7500	-6.0543	-10.0450	-5.0625	4.5000
$D_{NA,n}^{(2),s}$	-28.2865	-5.2693	5.9167	-0.4583	34.4008	-7.3623	-12.9375	1.3750
$D_{l,n}^{(2),s}$	15.5016	-0.5273	-1.8333	0.1667	-21.3855	9.3091	3.7500	-0.5000
$D_{F,n}^{(2),s}$	-10.1876	6.3423	-1.8333	0.1667	18.5432	-14.2997	3.7500	-0.5000
$D_n^{(0),p}$	4.0000	-2.0000	0.0000	0.0000	1.0000	1.0000	0.0000	0.0000
$D_n^{(1),p}$	-2.9623	-4.5000	1.5000	0.0000	2.6062	-3.0000	-1.5000	0.0000
$D_{A,n}^{(2),p}$	1.0691	0.8578	3.5625	-0.7500	-5.6088	-6.8483	4.3125	1.5000
$D_{NA,n}^{(2),p}$	-17.6658	-5.2693	5.9167	-0.4583	6.0218	-13.6485	-2.4792	0.4583
$D_{l,n}^{(2),p}$	10.9195	-0.5273	-1.8333	0.1667	-0.9696	6.3253	0.5833	-0.1667
$D_{F,n}^{(2),p}$	-11.5909	6.3423	-1.8333	0.1667	0.8079	-3.5443	0.5833	-0.1667

Table 1: Numerical values for the coefficients D_n^δ at one-, two- and three-loop level for $\mu^2 = m^2$.

Although the calculation is performed analytically the results are listed in numerical form in Tab. 2 with the choice $\mu^2 = m^2$. The analytic expressions are given in App. C.

For the vector correlator the first seven coefficients are already listed in [6], whereas all other results are new.

Threshold behaviour

At threshold it is most convenient to consider first the information about $R^\delta(v)$ and transform this subsequently into the corresponding expression for $\Pi^\delta(q^2)$ via dispersion

δ	n	$C_n^{(0),\delta}$	$C_n^{(1),\delta}$	$C_{A,n}^{(2),\delta}$	$C_{NA,n}^{(2),\delta}$	$C_{l,n}^{(2),\delta}$	$C_{F,n}^{(2),\delta}$
v	1	1.06667	4.04938	5.07543	7.09759	-2.33896	0.72704
	2	0.45714	2.66074	6.39333	6.31108	-2.17395	0.26711
	3	0.27090	2.01494	6.68902	5.39768	-1.89566	0.14989
	4	0.18470	1.62997	6.68456	4.69907	-1.67089	0.09947
	5	0.13640	1.37194	6.57434	4.16490	-1.49436	0.07230
	6	0.10609	1.18616	6.42606	3.74591	-1.35348	0.05566
	7	0.08558	1.04568	6.26672	3.40886	-1.23871	0.04459
	8	0.07094	0.93558	6.10789	3.13175	-1.14341	0.03677
a	1	0.53333	1.70123	2.31402	2.71368	-1.04643	0.34325
	2	0.15238	0.71577	1.64824	1.69284	-0.66383	0.06509
	3	0.06772	0.39678	1.18988	1.09011	-0.43131	0.02238
	4	0.03694	0.25243	0.89978	0.75793	-0.30145	0.01013
	5	0.02273	0.17477	0.70769	0.55831	-0.22280	0.00540
	6	0.01516	0.12819	0.57409	0.42925	-0.17167	0.00320
	7	0.01070	0.09805	0.47720	0.34095	-0.13656	0.00205
	8	0.00788	0.07743	0.40449	0.27780	-0.11138	0.00139
s	1	0.80000	0.45185	0.03484	-2.51105	0.88148	0.71856
	2	0.22857	0.77651	1.42576	0.89546	-0.35912	0.19112
	3	0.10159	0.52152	1.52607	0.99889	-0.40023	0.07144
	4	0.05541	0.35707	1.32709	0.82750	-0.33359	0.03362
	5	0.03410	0.25650	1.11491	0.66459	-0.26913	0.01832
	6	0.02273	0.19215	0.93714	0.53778	-0.21845	0.01103
	7	0.01605	0.14892	0.79516	0.44174	-0.17982	0.00715
	8	0.01182	0.11862	0.68238	0.36853	-0.15024	0.00489
p	1	1.33333	2.33333	2.71218	-1.85805	0.92593	1.31106
	2	0.53333	2.61481	7.03952	3.57843	-1.23162	0.49637
	3	0.30476	2.12783	8.27333	4.10409	-1.50248	0.25889
	4	0.20317	1.75361	8.46632	3.93931	-1.47479	0.16180
	5	0.14776	1.48309	8.33148	3.65904	-1.38655	0.11237
	6	0.11366	1.28241	8.09038	3.38071	-1.29093	0.08353
	7	0.09093	1.12869	7.82133	3.13004	-1.20154	0.06509
	8	0.07488	1.00753	7.55403	2.91007	-1.12143	0.05249

Table 2: Numerical values for the coefficients C_n^δ at one-, two- and three-loop level for $\mu^2 = m^2$.

relations. Whereas the treatment of the four cases in the high energy and small q^2 region is quite similar there is a big difference at threshold between the vector and pseudo-scalar correlators on one hand and the axial-vector and scalar correlators on the other hand. The latter are suppressed by a factor v^2 w.r.t. the former. This can already be seen by

considering the Born results:

$$R^{(0),v} = 3\frac{v\,(3-v^2)}{2}, \quad R^{(0),a} = 3v^3, \quad R^{(0),s} = 3v^3, \quad R^{(0),p} = 3v. \tag{13}$$

At $\mathcal{O}(\alpha_s)$ an expansion for $v \to 0$ is helpful for the considerations below. It reads:

$$R^{(1),v} = R^{(0),v}\left(\frac{\pi^2\,(1+v^2)}{2v} - 4\right) + \mathcal{O}(v^3), \tag{14}$$

$$R^{(1),a} = R^{(0),a}\left(\frac{\pi^2\,(1+v^2)}{2v} - 2\right) + \mathcal{O}(v^5), \tag{15}$$

$$R^{(1),s} = R^{(0),s}\left(\frac{\pi^2\,(1+v^2)}{2v} - 1\right) + \mathcal{O}(v^5), \tag{16}$$

$$R^{(1),p} = R^{(0),p}\left(\frac{\pi^2\,(1+v^2)}{2v} - 3\right) + \mathcal{O}(v^3). \tag{17}$$

The exact results can be found in [11, 12]. The analytical evaluation of the double-bubble diagrams with massless fermion loop insertions indicates [13] that the characteristic scale of the first two terms proportional to π^2 is given by the relative momentum, the last term (which is due to hard transversal gluon exchange) by the mass of the heavy fermion. This motivates the decomposition adopted in Eqs. (14-17).

Let us at $\mathcal{O}(\alpha_s^2)$ first discuss the abelian contribution proportional to C_F^2. The ratio between $R_A^{(2),\delta}$ and $R^{(0),\delta}$ is proportional to the Sommerfeld factor $y/(1-e^{-y})$ with $y = C_F\pi\alpha_s/v$, which resums contributions of the form $(\alpha_s/v)^n$. Axial-vector and scalar correlators follow the P-wave scattering solution for the Coulomb potential. Hence an additional factor $(1+y^2/(4\pi^2))$ has to be taken into account in order to obtain the correct leading term of $\mathcal{O}(\alpha_s^2)$ [14]. For the vector and pseudo-scalar contribution also the next-to-leading term in v can be determined by taking into account the correction factor arising from the exchange of transversal gluons which reads $(1-C_F4\alpha_s/\pi)$ for the vector and $(1-C_F3\alpha_s/\pi)$ for the pseudo-scalar case. As $R_A^{(2),a}$ and $R_A^{(2),s}$ already start at $\mathcal{O}(v)$ the corresponding factors are not considered. Finally we arrive at

$$R_A^{(2),v} = 3\left(\frac{\pi^4}{8v} - 3\pi^2\right) + \mathcal{O}(v), \qquad R_A^{(2),a} = 3\left(\frac{\pi^2(3+\pi^2)}{12}v\right) + \mathcal{O}(v^2), \tag{18}$$

$$R_A^{(2),s} = 3\left(\frac{\pi^2(3+\pi^2)}{12}v\right) + \mathcal{O}(v^2), \qquad R_A^{(2),p} = 3\left(\frac{\pi^4}{12v} - \frac{3}{2}\pi^2\right) + \mathcal{O}(v). \tag{19}$$

It is, of course, necessary to incorporate the strong $1/v$ singularity into the approximation method for the vector and pseudo-scalar case. In contrast the axial-vector and scalar current correlator are very smooth at threshold so that these terms are not used for our procedure. The comparison of these Padé results with the exact terms at threshold will be performed in Section 4 and demonstrates that the threshold behaviour is well reproduced — an independent test of our method.

The analytical results for the three-loop diagrams where a massless quark loop is inserted into the gluon propagator plus the corresponding real corrections are available for the vector current correlator [13] and the remaining correlators as well[2] [15] in analytic form. The scalar case can also be found in [16]. Expanding the results near threshold leads to

$$R_l^{(2),v} = R^{(0),v}\,\frac{\pi^2\,(1+v^2)}{v}\left(\frac{1}{6}\ln\frac{v^2 s}{\mu^2}-\frac{5}{18}\right)+\mathcal{O}(v), \tag{20}$$

$$R_l^{(2),a} = R^{(0),a}\,\frac{\pi^2\,(1+v^2)}{v}\left(\frac{1}{6}\ln\frac{v^2 s}{\mu^2}-\frac{11}{18}\right)+\mathcal{O}(v^3), \tag{21}$$

$$R_l^{(2),s} = R^{(0),a}\,\frac{\pi^2\,(1+v^2)}{v}\left(\frac{1}{6}\ln\frac{v^2 s}{\mu^2}-\frac{11}{18}\right)+\mathcal{O}(v^3), \tag{22}$$

$$R_l^{(2),p} = R^{(0),p}\,\frac{\pi^2\,(1+v^2)}{v}\left(\frac{1}{6}\ln\frac{v^2 s}{\mu^2}-\frac{5}{18}\right)+\mathcal{O}(v). \tag{23}$$

We include subleading terms proportional to $\ln v$ in this expansion, since the agreement of our approximation improves visibly in those cases where the analytical result is known.

In order to get the threshold behaviour for the non-abelian part it is either possible to use the QCD potential and the perturbative relation between $\alpha_V(\vec{q}^{\,2})$ and $\alpha_s(\mu^2)$ or to proceed as demonstrated in [17] and deduce the gluonic double-bubble diagram, $R_g^{(2),\delta}$, from the corresponding fermionic contribution and evaluate it for a special choice of the gauge parameter ξ. This is based on the observation that the terms proportional to C_A in the relation between $\alpha_V(\vec{q}^{\,2})$ and $\alpha_s(\mu^2)$ are covered by the (one-loop) gluon propagator choosing $\xi = 4$. We will choose the second method since this trick is used also for the actual calculation. Following [6] the expansion of the "double-bubble" result for $\xi = 4$ is taken to represent the expansion of the full non-abelian part. For the four correlators it is given by:

$$R_{NA}^{(2),v} = R^{(0),v}\,\frac{\pi^2\,(1+v^2)}{v}\left(-\frac{11}{24}\ln\frac{v^2 s}{\mu^2}+\frac{31}{72}\right)+\mathcal{O}(v), \tag{24}$$

$$R_{NA}^{(2),a} = R^{(0),a}\,\frac{\pi^2\,(1+v^2)}{v}\left(-\frac{11}{24}\ln\frac{v^2 s}{\mu^2}+\frac{97}{72}\right)+\mathcal{O}(v^3), \tag{25}$$

$$R_{NA}^{(2),s} = R^{(0),s}\,\frac{\pi^2\,(1+v^2)}{v}\left(-\frac{11}{24}\ln\frac{v^2 s}{\mu^2}+\frac{97}{72}\right)+\mathcal{O}(v^3), \tag{26}$$

$$R_{NA}^{(2),p} = R^{(0),p}\,\frac{\pi^2\,(1+v^2)}{v}\left(-\frac{11}{24}\ln\frac{v^2 s}{\mu^2}+\frac{31}{72}\right)+\mathcal{O}(v). \tag{27}$$

To combine the results from different kinematical regions the above expressions for the imaginary part have to be transformed into analytical functions for $\Pi^\delta(q^2)$ which respect Eqs. (6) and (7). This can be done in close analogy to [6].

[2]We would like to thank the authors of [15] for providing their results prior to publication.

3 The approximation procedure

This section is devoted to the description of the approximation method. In order to save space we will not present explicit formulae. They look very similar to the ones for the vector case discussed in [6]. The treatment of the abelian part of the pseudo-scalar correlator is in close analogy to [18].

In a first step a function $\tilde{\Pi}^\delta(q^2)$ is constructed which contains no high energy singularities and no logarithmic terms at threshold. This is achieved with the help of the function

$$G(z) = \frac{2u \ln u}{u^2 - 1}, \qquad u = \frac{\sqrt{1 - 1/z} - 1}{\sqrt{1 - 1/z} + 1}. \tag{28}$$

The combination $(1-z)G(z)$ has a polynomial behaviour for $z \to 0$ and vanishes at threshold ($z \to 1$). For the case $z \to -\infty$ the expansion of $G(z)$ develops logarithms starting with $\ln(-1/(4z))/(2z)$. This property is exploited and a function of the form

$$\sum_{n,m,l} c_{nml}\, z^n (1-z)^m \left(G(z)\right)^l, \tag{29}$$

where n is an integer and $m, l \geq 0$ is constructed in order to remove the $\ln(-z)$ terms of $\Pi^\delta(q^2)$. Whereas for the vector case described in [6] no cubic logarithms appear (see Tab. 1) and therefore quadratic combinations in $G(z)$ are sufficient, for the other three cases this is not true: The axial-vector correlator develops $\ln^3(-z)/z$ terms and combinations like $(1-z)^2(G(z))^3$ are required. For the scalar and pseudo-scalar case also cubic logarithms appear which are not suppressed by powers of z, whence terms like $z(1-z)^2(G(z))^3$ must appear in the expression subtracted from $\Pi^\delta(q^2)$.

If logarithmic terms are present near threshold ($\Pi_{NA}^{(2),\delta}$ and $\Pi_l^{(2),\delta}$) they are first subtracted and then the high energy singularities are removed. For the abelian polarization function where either $1/v$ singularities ($\Pi_A^{(2),v}$ and $\Pi_A^{(2),p}$) or just constant terms ($\Pi_A^{(2),a}$ and $\Pi_A^{(2),s}$) are present for $z \to 1$ only the high energy logarithms are removed.

In a second step we perform a variable change. Via the conformal mapping

$$\omega = \frac{1 - \sqrt{1 - q^2/4m^2}}{1 + \sqrt{1 - q^2/4m^2}}, \qquad z = \frac{q^2}{4m^2} = \frac{4\omega}{(1+\omega)^2}. \tag{30}$$

the complex q^2-plane is mapped into the interior of the unit circle and the upper (lower) part of the cut starting at $z = 1$ is mapped onto the upper (lower) perimeter of the circle. The special points $q^2 = 0, 4m^2, -\infty$ correspond to $\omega = 0, 1, -1$, respectively. In this new variable we construct a function $P(\omega)$ for which the Padé approximation is performed. According to the different behaviour of $\tilde{\Pi}^\delta(q^2)$ near threshold actually two different functions have to be defined:

$$P^I(\omega) = \frac{1-\omega}{(1+\omega)^2}\left(\tilde{\Pi}(q^2) - \tilde{\Pi}(-\infty)\right), \tag{31}$$

$$P^{II}(\omega) = \frac{1}{(1+\omega)^2}\left(\tilde{\Pi}(q^2) - \tilde{\Pi}(-\infty)\right). \tag{32}$$

Thereby $P^I(\omega)$ takes care of the cases where a $1/v$ singularity is present ($\Pi_A^{(2),v}$ and $\Pi_A^{(2),p}$). The factor $(1-\omega)$ corresponds effectively to a multiplication with v. At this point we should mention that in order to incorporate also the constant term at threshold which has its origin in the correction factor introduced before Eq. (18) the combinations $\Pi_A^{(2),v} + 4\Pi^{(1),v}$ and $\Pi_A^{(2),p} + 3\Pi^{(1),p}$ are considered. The two-loop results $\Pi^{(1),v}$ and $\Pi^{(1),p}$ may be found in [19] and [20], respectively.

$P^{II}(\omega)$ treats all other cases where $\tilde{\Pi}^\delta(q^2)$ is just a constant for $z = 1$. Note, that this constant is unknown and consequently $P^{II}(1)$ may not be used for the construction of the Padé approximation. $P^I(1)$ is directly connected with the $1/v$ singularity and, of course, known. The high energy terms are treated in the same way for $P^I(\omega)$ and $P^{II}(\omega)$: Due to the subtraction of $\tilde{\Pi}^\delta(-\infty)$ the constant terms transform to $P(0)$ and the difference together with the prefactor $1/(1+\omega)^2$ projects out the $1/z$ suppressed terms in the limit $\omega \to -1$. Finally the moments from $z \to 0$ transform into derivatives of $P(\omega)$ at $\omega = 0$. In total the following information is available for $P^I(\omega)$: $\{P^I(-1), P^I(0), P^{I,(1)}(0), \ldots, P^{I,(8)}(0), P^I(1)\}$. These eleven data points allow the construction of Padé approximations like [5/5], [6/4] or [4/6]. For $P^{II}(\omega)$ the threshold information $P^{II}(1)$ is not available which means that at most Padé approximations like [5/4] or [4/5] may be constructed.

For the non-abelian contributions proportional to $C_A C_F$ there is an alternative approach. Following the method outlined in [17] the imaginary part of the gluonic double-bubble contributions, $R_g^{(2),\delta}(s)$, can be computed analytically from the knowledge of the fermionic contribution $R_l^{(2),\delta}(s)$. $R_g^{(2),\delta}(s)$ is, of course, gauge dependent. However, for the special choice $\xi = 4$, where ξ is defined via the gluon propagator $(-g^{\mu\nu} + \xi\, q^\mu\, q^\nu/q^2)/(q^2 + i\epsilon)$ the threshold behaviour of the non-abelian contribution (see Eqs. (24-27)) and the leading high energy logarithms are covered by $R_g^{(2),\delta}(s)$. Therefore it is promising to apply the procedure described above to the difference $\Pi_{NA}^{(2),\delta}(q^2) - \Pi_g^{(2),\delta}(q^2)|_{\xi=4}$ which has a less singular behaviour than $\Pi_{NA}^{(2),\delta}(q^2)$. The results for the non-abelian contribution presented in the next section are based on this method.

4 Results

After the Padé approximation is performed for the function $P(\omega)$ the corresponding equations are inverted in order to get $\Pi^\delta(q^2)$. In Figs. 1–4 the results are presented grouped according to the threshold behaviour. In Fig. 1 and 3 $R(s)$ is plotted against the velocity for the vector and pseudo-scalar and the axial-vector and scalar case, respectively. The Figs. 2 and 4 contain the corrections plotted versus x. Also the threshold and high energy approximations are shown (dashed lines). For the vector correlator terms up to $\mathcal{O}(x^{12})$ are available [4]. Although in our procedure only terms up to $\mathcal{O}(x^2)$ are incorporated the higher order terms are very well reproduced. For the scalar and pseudo-scalar polarization function terms up to $\mathcal{O}(x^8)$ are available [5]. Again only the quadratic terms are build into the approximation method. However, the numerical coincidence with the high energy approximations is very good. Actually it is hardly possible to detect a difference

between the high energy terms and the Padé results when x is used as abscissa. A similar behaviour is observed for the axial-vector case where only quartic terms are available [21].

In this presentation it is not possible to notice any difference between the different Padé approximants. Minor differences can be seen after the leading terms at threshold are subtracted. This can be seen in Figs. 5 and 6. It should be stressed that the vertical scale is expanded by up to a factor 100 in comparison with Figs. 1 and 3. The following notation is adopted: All Padé approximations containing information up to C_6 are plotted as a dashed line and the higher ones as full lines. The obvious exceptions are represented by a dash-dotted line and the exact results are drawn as dotted curves.

The vector case is already discussed in [6]. The inclusion of C_8 into the analysis shows a further stabilization of the results. The plot for the abelian part in Fig. 5 contains altogether 14 Padé approximations. Eight of them contain information up to C_6 (dashed lines), and six contain also information from C_7 and C_8. These latter six lines coincide even on the expanded scale. The dash-dotted curve belongs to the [2/5] result and contains a pole for $\omega \approx 1.06$. In the case of the non-abelian contribution 15 Padé approximations are plotted. Again the dashed lines belong to the lower order results. The dash-dotted curves are the results of two Padé approximants which have poles close to $\omega = 1$ ($[4/3] : \omega \approx 1.07$ and $[2/5] : \omega \approx 1.06$).

For the pseudo-scalar correlator we find similar results concerning the behaviour of the Padé approximations when more information is included. The abelian contribution for the pseudo-scalar case contains 17 different results. The dash-dotted lines differ from the remaining ones significantly. The corresponding Padé approximants are [3/2] and [2/5]. A spread between the different Padé approximants can also be observed for the non-abelian contribution to the vector and pseudo-scalar cases. In both cases, however, convergence is visible if more information is included into the construction procedure. In the plot for $\delta R_{NA}^{(2),p}(s)$, e.g., the dash-dotted line correspond to the Padé approximation [2/3] containing only the first three moments for $q^2 \to 0$. If this curve is ignored the spread is much less dramatic and the difference between the remaining Padé approximations shown is very tiny and completely negligible. The excellent agreement for the fermionic contribution in the pseudo-scalar case is comparable to the one for the vector correlator. In both cases the exact results [15], plotted as a dotted line, is indistinguishable from the approximations.

Coming to the axial-vector and scalar case we would like to remind the reader that for these correlators no singularities are present in the limit $v \to 0$. However, also here it is instructive to subtract the leading terms and look closer to the remainders $\delta R^{(2),a}$ and $\delta R^{(2),s}$. As can be seen by comparing Fig. 3 and Fig. 6 the reduction in the scale lies between a factor two and ten. Also the very smooth behaviour of the subtracted results near threshold is clearly visible. One recognizes that, e.g. the remainders of the non-abelian and light-fermion contributions shown in Fig. 6 are zero almost up to $v \approx 0.2$.

Let us now consider the threshold behaviour of the abelian contribution. As mentioned in Section 2 the corrections start with a term linear in v. We are now in the position to compare the Padé results with the exact expressions. In Tab. 3 the numerical values of the coefficients of both the expansion and the exact result is shown. Although the

P.A.	$R_A^{(2),a}$	P.A.	$R_A^{(2),s}$
[3/2]	29.56	[3/3]	31.31
[2/3]	29.59	[4/2]	31.31
[3/3]	29.64	[2/4]	31.44
[4/2]	29.69	[3/4]	31.38
[2/4]	29.63	[5/2]	31.39
[2/5]	29.77	[2/5]	31.39
[3/5]	29.96	[6/3]	31.22
[6/2]	30.14	[3/6]	31.28
[2/6]	29.82		
[5/4]	31.23		
[4/5]	31.71		
[6/3]	32.55		
exact	31.75	exact	31.75

Table 3: Comparison of the leading term at threshold for $R_A^{(2),\delta}$ ($\delta = a, s$) with the exact expression. All Padé approximants (P.A.) contain two terms from the high energy region as input. Only the number of moments from the expansion $q^2 \to 0$ is different.

analytically known terms are not incorporated into the approximation method they are very well reproduced by our method.

In the abelian part of the scalar correlator there are two Padé approximants which differ significantly (dash-dotted lines) from the other eight results. One of them is a low-order Padé approximation containing only the information up to C_2 and the other one ([4/3]) has a pole close to $\omega = 1$ (1.02) which is reflected in the enhancement in the vicinity of the threshold.

Both the non-abelian and fermionic contributions show an excellent agreement between the different Padé approximations. We should mention that at least 14 approximations are plotted and for $R_l^{(2),a}(s)$ and $R_l^{(2),s}(s)$ in addition the exact results are included. Again no differences are visible.

Finally we present handy approximation formulae for the abelian and non-abelian contributions. The procedure used to get them is described in [6]. There the approximation formulae for the vector case are already listed. For completeness we repeat them at this point:

$$\begin{aligned} R_A^{(2),v} &= \frac{(1-v^2)^4}{v}\frac{3\pi^4}{8} - 4R^{(1),v} + v\frac{2619}{64} - v^3\frac{2061}{64} + \frac{81}{8}\left(1-v^2\right)\ln\frac{1-v}{1+v} \\ &\quad - 198\left(\frac{m^2}{s}\right)^{3/2}\left(v^4-2v^2\right)^6 \\ &\quad + 100p^{3/2}(1-p)\left[2.21\,P_0(p) - 1.57\,P_1(p) + 0.27\,P_2(p)\right], \end{aligned} \tag{33}$$

$$
\begin{aligned}
R_{NA}^{(2),v} &= R_g^{(2),v}\Big|_{\xi=4} + v\frac{351}{32} - v^3\frac{297}{32} \\
&\quad - 18\left(\frac{m^2}{s}\right)^{3/2}\left(v^4-2v^2\right)^4 \\
&\quad + 50p^{3/2}(1-p)\left[1.73\,P_0(p) - 1.24\,P_1(p) + 0.64\,P_2(p)\right], \qquad (34)
\end{aligned}
$$

$$
\begin{aligned}
R_{A}^{(2),a} &= -\frac{585}{32}v + 18v^3 + \left(\left(27v-27v^3\right)(1-\ln 2)\right)\zeta(2) + \left(\frac{135}{8}\left(v-v^3\right)\right)\zeta(3) \\
&\quad + \left(-\frac{189}{32}\left(1-v^2\right)\right)\ln\frac{1-v}{1+v} + \left(-\frac{81}{16}\left(v-v^3\right)\right)\ln^2\frac{1-v}{1+v} \\
&\quad + 50p^{3/2}(1-p)\left[11.97\,P_0(p) - 25.37\,P_1(p) + 20.67\,P_2(p)\right. \\
&\qquad \left. - 9.048\,P_3(p) + 1.85\,P_4(p)\right], \qquad (35) \\
R_{NA}^{(2),a} &= R_g^{(2),a}\Big|_{\xi=4} - \frac{9}{16}v + \frac{9}{4}v^3 + \left(\left(-\frac{135}{8}+\frac{27}{2}\ln 2\right)\left(v-v^3\right)\right)\zeta(2) \\
&\quad + \left(\frac{27}{16}\left(v-v^3\right)\right)\zeta(3) + \left(-\frac{135}{16}\left(1-v^2\right)\right)\ln\frac{1-v}{1+v} \\
&\quad + 50p^{3/2}(1-p)\left[-1.88P_0(p) + 3.31P_1(p) - 1.96P_2(p) + 0.483P_3(p)\right], \qquad (36)
\end{aligned}
$$

$$
\begin{aligned}
R_{A}^{(2),s} &= -\frac{1125}{64}v + \frac{1779}{64}v^3 + \left(\frac{189}{4}v - \frac{261}{4}v^3 + \left(-27v+45v^3\right)\ln 2\right)\zeta(2) \\
&\quad + \left(\frac{189}{8}v - \frac{279}{8}v^3\right)\zeta(3) + \left(-\frac{63}{8}+\frac{297}{16}v^2\right)\ln\frac{1-v}{1+v} \\
&\quad + \left(-\frac{243}{16}v + \frac{297}{16}v^3\right)\ln^2\frac{1-v}{1+v} \\
&\quad + 240\left(\frac{m^2}{s}\right)^{3/2}\left(v^4-2v^2\right)^4 \\
&\quad + 50p^{3/2}(1-p)\left[1.30\,P_0(p) - 4.37\,P_1(p) + 3.58\,P_2(p) - 0.91\,P_3(p)\right], \qquad (37) \\
R_{NA}^{(2),s} &= R_g^{(2),s}\Big|_{\xi=4} + \frac{99}{32}v + \frac{147}{32}v^3 + \left(-\frac{135}{8}v + \frac{225}{8}v^3 + \left(\frac{27}{2}v - \frac{45}{2}v^3\right)\ln 2\right)\zeta(2) \\
&\quad + \left(-\frac{27}{16}v + \frac{9}{16}v^3\right)\zeta(3) + \left(-\frac{45}{4}+\frac{135}{8}v^2\right)\ln\frac{1-v}{1+v} \\
&\quad + 50p^{3/2}(1-p)\left[-3.94\,P_0(p) + 6.97\,P_1(p) - 4.11\,P_2(p) + 1.00\,P_3(p)\right], \qquad (38)
\end{aligned}
$$

$$
\begin{aligned}
R_{A}^{(2),p} &= +\frac{(1-v^2)^4}{v}\frac{\pi^4}{4} - 3R^{(1),p} + \frac{2763}{64}v - \frac{813}{64}v^3 + \left(-\frac{9}{4}v - \frac{63}{4}v^3\right. \\
&\quad \left. + \left(9v+9v^3\right)\ln 2\right)\zeta(2) + \left(-\frac{27}{8}v - \frac{63}{8}v^3\right)\zeta(3) \\
&\quad + \left(\frac{81}{4}+\frac{63}{16}v^2\right)\ln\frac{1-v}{1+v} + \left(-\frac{27}{16}v + \frac{81}{16}v^3\right)\ln^2\frac{1-v}{1+v} \\
&\quad - 300\left(\frac{m^2}{s}\right)^{3/2}\left(v^4-2v^2\right)^6
\end{aligned}
$$

$$+ 100p^{3/2}(1-p)\left[2.79\,P_0(p) - 1.83\,P_1(p) + 0.419\,P_2(p)\right], \tag{39}$$

$$\begin{aligned} R_{NA}^{(2),p} &= R_g^{(2),p}\Big|_{\xi=4} + \frac{459}{32}v - \frac{213}{32}v^3 + \left(\frac{45}{8} - \frac{9}{2}\ln 2\right)\left(v + v^3\right)\zeta(2) \\ &+ \left(-\frac{27}{16}v + \frac{9}{16}v^3\right)\zeta(3) + \frac{45}{8}v^2\ln\frac{1-v}{1+v} \\ &+ 12\left(\frac{m^2}{s}\right)^{3/2}\left(v^4 - 2v^2\right)^4 \\ &+ 50p^{3/2}(1-p)\left[0.354\,P_0(p) - 0.251\,P_1(p) + 0.456\,P_2(p)\right], \end{aligned} \tag{40}$$

where $p = (1-v)/(1+v)$, $\zeta(2) = \pi^2/6$, $\zeta(3) \approx 1.20206$ and $P_i(p)$ are the Legendre polynoms:

$$P_0(p) = 1, \;\; P_1(p) = p, \;\; P_2(p) = -\frac{1}{2} + \frac{3}{2}p^2, \tag{41}$$

$$P_3(p) = -\frac{3}{2}p + \frac{5}{2}p^3, \;\; P_4(p) = \frac{3}{8} - \frac{15}{4}p^2 + \frac{35}{8}p^4. \tag{42}$$

$R_g^{(2),\delta}$ is the exact result for the gluonic double-bubble to be reconstructed from the fermionic contribution [17]:

$$R_g^{(2),\delta}\Big|_{\xi=4} = -\frac{11}{4}R_l^{(2),\delta} - \frac{2}{3}R^{(1),\delta}. \tag{43}$$

For some cases the degree of the polynomial used for the fit has to be increased in order to end up with reasonable approximations. The first lines of the result contain the exactly known high energy and threshold contributions. The proceeding lines represent the numerically small remainder, $R_x^{(2),\delta,rem}$ with $x \in \{A, NA\}$, which is plotted in Fig. 7 together with the result from the Padé approximation.

5 Conclusions and summary

The vacuum polarization function has been evaluated in order α_s^2 for vector, axial-vector, scalar and pseudo-scalar currents. The results take full account of the quark mass and are applicable between the production threshold and the high energy region. The method is based on the Padé approximation and uses the leading terms at high energies and at threshold plus the lowest eight coefficients of the Taylor series of $\Pi^\delta(q^2)$ around zero. The stability of this approximation has been verified and excellent agreement between the present result and the predictions based on the high energy expansion is observed. These results can be used to evaluate the cross section for top pair production in electron positron annihilation through the vector and axial-vector current and the decay rate of a scalar or pseudo-scalar Higgs boson into top quarks in the full kinematical region and in next-to-leading order.

Acknowledgments

We would like to thank A.H. Hoang and T. Teubner for interesting discussions and for providing us with the analytic results for $R_l^{(2),\delta}$ prior to publication which were crucial for our tests of the approximation methods.

Appendix

A $\overline{\rm MS}$ definition of the polarization functions

In this appendix we present the missing pieces needed to express the polarization functions, $\Pi^\delta(q^2)$, in the $\overline{\rm MS}$ scheme which means that in the expression obtained after the renormalization of α_s and m only the poles are subtracted. Expressing the results still in terms of the on-shell mass, m, $\bar\Pi^\delta(q^2)$ reads:

$$\bar\Pi^\delta(q^2) \;=\; \frac{3}{16\pi^2}\left[\bar C^\delta_{-1}\frac{1}{z}+\bar C^\delta_0\right]+\Pi^\delta(q^2), \tag{A.1}$$

where the bar only refers to the overall renormalization. For the different cases we get ($\bar C_0^v$ is already listed in [6]):

$$\begin{aligned}
\bar C_0^v \;=\;& \frac{4}{3}L_{\mu m}+\frac{\alpha_s}{\pi}C_F\left(\frac{15}{4}+L_{\mu m}\right)\\
&+\left(\frac{\alpha_s}{\pi}\right)^2\left[C_F^2\left(\frac{77}{144}-\frac{1}{8}L_{\mu m}+(5-8\ln 2)\zeta(2)+\frac{1}{48}\zeta(3)\right)\right.\\
&+C_FC_A\left(\frac{14977}{2592}+\frac{157}{36}L_{\mu m}+\frac{11}{24}L_{\mu m}^2+(-\frac{4}{3}+4\ln 2)\zeta(2)+\frac{127}{96}\zeta(3)\right)\\
&+C_FTn_l\left(-\frac{917}{648}-\frac{14}{9}L_{\mu m}-\frac{1}{6}L_{\mu m}^2-\frac{4}{3}\zeta(2)\right)\\
&\left.+C_FT\left(-\frac{695}{162}-\frac{14}{9}L_{\mu m}-\frac{1}{6}L_{\mu m}^2+\frac{8}{3}\zeta(2)+\frac{7}{16}\zeta(3)\right)\right],
\end{aligned} \tag{A.2}$$

$$\bar C_{-1}^v \;=\; 0, \tag{A.3}$$

$$\begin{aligned}
\bar C_0^a \;=\;& -\frac{4}{3}+\frac{4}{3}L_{\mu m}+\frac{\alpha_s}{\pi}C_F\left(\frac{67}{36}+L_{\mu m}\right)\\
&+\left(\frac{\alpha_s}{\pi}\right)^2\left[C_F^2\left(\frac{131}{54}-\frac{1}{8}L_{\mu m}+(5-8\ln 2)\zeta(2)+\frac{115}{288}\zeta(3)\right)\right.\\
&+C_FC_A\left(\frac{4081}{432}+\frac{71}{27}L_{\mu m}+\frac{11}{24}L_{\mu m}^2+(-\frac{4}{3}+4\ln 2)\zeta(2)-\frac{883}{576}\zeta(3)\right)\\
&+C_FTn_l\left(-\frac{149}{72}-\frac{25}{27}L_{\mu m}+-\frac{1}{6}L_{\mu m}^2-\frac{4}{3}\zeta(2)\right)\\
&\left.+C_FT\left(-\frac{55}{12}-\frac{25}{27}L_{\mu m}-\frac{1}{6}L_{\mu m}^2+\frac{8}{3}\zeta(2)-\frac{7}{48}\zeta(3)\right)\right],
\end{aligned} \tag{A.4}$$

$$\bar C_{-1}^a \;=\; -2L_{\mu m}+\frac{\alpha_s}{\pi}C_F\left(-\frac{33}{8}+\frac{3}{2}L_{\mu m}+\frac{3}{2}L_{\mu m}^2\right)$$

$$
\begin{aligned}
&+\left(\frac{\alpha_s}{\pi}\right)^2\left[C_F^2\left(\frac{529}{64}-\frac{3}{2}B_4+\frac{13}{2}L_{\mu m}-\frac{15}{16}L_{\mu m}^2-\frac{3}{4}L_{\mu m}^3\right.\right.\\
&\quad\left.+\left(-\frac{15}{2}+12\ln 2\right)(1-L_{\mu m})\,\zeta(2)+\left(-12-\frac{3}{2}L_{\mu m}\right)\zeta(3)+\frac{27}{4}\zeta(4)\right)\\
&+C_FC_A\left(-\frac{1039}{96}+\frac{3}{4}B_4+\frac{143}{48}L_{\mu m}+\frac{109}{24}L_{\mu m}^2+\frac{11}{12}L_{\mu m}^3\right.\\
&\quad\left.+(2-6\ln 2)(1-L_{\mu m})\,\zeta(2)+\left(\frac{23}{6}+\frac{3}{4}L_{\mu m}\right)\zeta(3)-\frac{27}{8}\zeta(4)\right)\\
&+C_FTn_l\left(\frac{35}{12}-\frac{7}{12}L_{\mu m}-\frac{4}{3}L_{\mu m}^2-\frac{1}{3}L_{\mu m}^3+(2-2L_{\mu m})\,\zeta(2)+\frac{4}{3}\zeta(3)\right)\\
&+C_FT\left(\frac{59}{12}-\frac{43}{12}L_{\mu m}-\frac{4}{3}L_{\mu m}^2-\frac{1}{3}L_{\mu m}^3+(-4+4L_{\mu m})\,\zeta(2)+\frac{7}{12}\zeta(3)\right)\Bigg], \qquad \text{(A.5)}
\end{aligned}
$$

$$
\begin{aligned}
\bar{C}_0^s \;=\;& -\frac{4}{3}+2L_{\mu m}+\frac{\alpha_s}{\pi}C_F\left(\frac{41}{8}-\frac{3}{2}L_{\mu m}+-\frac{3}{2}L_{\mu m}^2\right)\\
&+\left(\frac{\alpha_s}{\pi}\right)^2\left[C_F^2\left(-\frac{505}{64}+\frac{3}{2}B_4-\frac{13}{2}L_{\mu m}+\frac{15}{16}L_{\mu m}^2+\frac{3}{4}L_{\mu m}^3\right.\right.\\
&\quad\left.+\left(\frac{25}{2}-20\ln 2\right)\left(1-\frac{3}{5}L_{\mu m}\right)\zeta(2)+\left(\frac{93}{8}+\frac{3}{2}L_{\mu m}\right)\zeta(3)-\frac{27}{4}\zeta(4)\right)\\
&+C_FC_A\left(\frac{5429}{288}-\frac{3}{4}B_4-\frac{33}{16}L_{\mu m}-\frac{109}{24}L_{\mu m}^2-\frac{11}{12}L_{\mu m}^3\right.\\
&\quad\left.+\left(-\frac{10}{3}+10\ln 2\right)\left(1-\frac{3}{5}L_{\mu m}\right)\zeta(2)+\left(-\frac{175}{48}-\frac{3}{4}L_{\mu m}\right)\zeta(3)+\frac{27}{8}\zeta(4)\right)\\
&+C_FTn_l\left(-\frac{191}{36}+\frac{1}{4}L_{\mu m}+\frac{4}{3}L_{\mu m}^2+\frac{1}{3}L_{\mu m}^3+\left(-\frac{10}{3}+2L_{\mu m}\right)\zeta(2)+-\frac{4}{3}\zeta(3)\right)\\
&+C_FT\left(-\frac{733}{72}+\frac{13}{4}L_{\mu m}+\frac{4}{3}L_{\mu m}^2+\frac{1}{3}L_{\mu m}^3+\left(\frac{20}{3}-4L_{\mu m}\right)\zeta(2)+-\frac{49}{48}\zeta(3)\right)\Bigg], \qquad \text{(A.6)}
\end{aligned}
$$

$$
\begin{aligned}
\bar{C}_{-1}^s \;=\;& -1-3L_{\mu m}+\frac{\alpha_s}{\pi}C_F\left(-\frac{9}{2}+9L_{\mu m}+\frac{9}{2}L_{\mu m}^2\right)\\
&+\left(\frac{\alpha_s}{\pi}\right)^2\left[C_F^2\left(\frac{1673}{64}-3B_4+\frac{45}{8}L_{\mu m}-\frac{207}{16}L_{\mu m}^2-\frac{9}{2}L_{\mu m}^3\right.\right.\\
&\quad\left.+\left(-\frac{15}{4}+6\ln 2\right)(1-6L_{\mu m})\,\zeta(2)-27\zeta(3)+\frac{27}{2}\zeta(4)\right)\\
&+C_AC_F\left(-\frac{2641}{192}+\frac{3}{2}B_4+\frac{163}{8}L_{\mu m}+\frac{251}{16}L_{\mu m}^2+\frac{11}{4}L_{\mu m}^3\right.\\
&\quad\left.+(1-3\ln 2)(1-6L_{\mu m})\,\zeta(2)+10\zeta(3)-\frac{27}{4}\zeta(4)\right)\\
&+C_FTn_l\left(\frac{161}{48}-\frac{11}{2}L_{\mu m}-\frac{19}{4}L_{\mu m}^2-L_{\mu m}^3+(1-6L_{\mu m})\,\zeta(2)+4\zeta(3)\right)\\
&+C_FT\left(\frac{99}{16}-\frac{23}{2}L_{\mu m}-\frac{19}{4}L_{\mu m}^2-L_{\mu m}^3+(-2+12L_{\mu m})\,\zeta(2)-\frac{7}{2}\zeta(3)\right)\Bigg], \qquad \text{(A.7)}
\end{aligned}
$$

$$
\begin{aligned}
\bar{C}_0^p &= 2L_{\mu m} + \frac{\alpha_s}{\pi} C_F \left(\frac{33}{8} - \frac{3}{2} L_{\mu m} + -\frac{3}{2} L_{\mu m}^2 \right) \\
&+ \left(\frac{\alpha_s}{\pi} \right)^2 \left[C_F^2 \left(-\frac{529}{64} + \frac{3}{2} B_4 + -\frac{13}{2} L_{\mu m} + \frac{15}{16} L_{\mu m}^2 + \frac{3}{4} L_{\mu m}^3 \right.\right. \\
&\quad \left.\left. + \left(\frac{15}{2} - 12 \ln 2 \right) (1 - L_{\mu m}) \zeta(2) + \left(12 + \frac{3}{2} L_{\mu m} \right) \zeta(3) + -\frac{27}{4} \zeta(4) \right) \right. \\
&+ C_A C_F \left(\frac{1039}{96} - \frac{3}{4} B_4 - \frac{143}{48} L_{\mu m} - \frac{109}{24} L_{\mu m}^2 - \frac{11}{12} L_{\mu m}^3 \right. \\
&\quad \left. + (-2 + +6 \ln 2) (1 - L_{\mu m}) \zeta(2) + \left(-\frac{23}{6} - \frac{3}{4} L_{\mu m} \right) \zeta(3) + \frac{27}{8} \zeta(4) \right) \\
&+ C_F T n_l \left(-\frac{35}{12} + \frac{7}{12} L_{\mu m} + \frac{4}{3} L_{\mu m}^2 + \frac{1}{3} L_{\mu m}^3 + (-2 + 2 L_{\mu m}) \zeta(2) - \frac{4}{3} \zeta(3) \right) \\
&+ C_F T \left(-\frac{59}{12} + \frac{43}{12} L_{\mu m} + \frac{4}{3} L_{\mu m}^2 + \frac{1}{3} L_{\mu m}^3 + (4 - 4 L_{\mu m}) \zeta(2) - \frac{7}{12} \zeta(3) \right) \Bigg], \qquad \text{(A.8)} \\
\bar{C}_{-1}^p &= -1 - L_{\mu m} + \frac{\alpha_s}{\pi} C_F \left(-\frac{1}{2} + 3 L_{\mu m} + \frac{3}{2} L_{\mu m}^2 \right) \\
&+ \left(\frac{\alpha_s}{\pi} \right)^2 \left[C_F^2 \left(\frac{1409}{192} - B_4 + \frac{15}{8} L_{\mu m} - \frac{69}{16} L_{\mu m}^2 - \frac{3}{2} L_{\mu m}^3 \right.\right. \\
&\quad \left.\left. + \left(\frac{15}{4} - 6 \ln 2 \right) (1 + 2 L_{\mu m}) \zeta(2) - 9 \zeta(3) + \frac{9}{2} \zeta(4) \right) \right. \\
&+ C_F C_A \left(-\frac{129}{64} + \frac{1}{2} B_4 + \frac{185}{24} L_{\mu m} + \frac{251}{48} L_{\mu m}^2 + \frac{11}{12} L_{\mu m}^3 \right. \\
&\quad \left. + (-1 + 3 \ln 2) (1 + 2 L_{\mu m}) \zeta(2) + \frac{10}{3} \zeta(3) - \frac{9}{4} \zeta(4) \right) \\
&+ C_F T n_l \left(\frac{19}{48} - \frac{13}{6} L_{\mu m} - \frac{19}{12} L_{\mu m}^2 - \frac{1}{3} L_{\mu m}^3 + (-1 - 2 L_{\mu m}) \zeta(2) + \frac{4}{3} \zeta(3) \right) \\
&+ C_F T \left(\frac{107}{48} - \frac{13}{6} L_{\mu m} - \frac{19}{12} L_{\mu m}^2 - \frac{1}{3} L_{\mu m}^3 + (2 + 4 L_{\mu m}) \zeta(2) - \frac{14}{3} \zeta(3) \right) \Bigg], \qquad \text{(A.9)}
\end{aligned}
$$

with $L_{\mu m} = \ln \mu^2/m^2$. ζ is Riemanns zeta-function with the values $\zeta(2) = \pi^2/6$, $\zeta(3) \approx 1.20206$, $\zeta(4) = \pi^4/90$, and $B_4 \approx -1.76280$ is a numerical constant typical for three-loop tadpole integrals [10].

B Analytic results for D_n^δ

For completeness we present in this appendix the analytical results for D_0^a and D_1^a.

$$
\begin{aligned}
D_0^{(0),a} &= \frac{32}{9} - \frac{4}{3} \ln \frac{-q^2}{m^2}, \qquad \text{(B.1)} \\
D_1^{(0),a} &= -2 + 2 \ln \frac{-q^2}{m^2}, \qquad \text{(B.2)}
\end{aligned}
$$

$$D_0^{(1),a} = \frac{49}{18} - 4\zeta(3) - \ln\frac{-q^2}{m^2}, \tag{B.3}$$

$$D_1^{(1),a} = -\frac{21}{4} + 6\zeta(3) + \frac{3}{2}\ln\frac{-q^2}{m^2} - \frac{3}{2}\ln^2\frac{-q^2}{m^2}, \tag{B.4}$$

$$\begin{aligned}
D_0^{(2),a} &= C_F^2\left(-\frac{953}{216} + 8\,\zeta(2)\,\ln 2 - 5\,\zeta(2) - \frac{1891}{288}\,\zeta(3) + 10\,\zeta(5) + \frac{1}{8}\,\ln\frac{-q^2}{m^2}\right) \\
&\quad + C_F\,C_A\left(\frac{19729}{2592} - 4\,\zeta(2)\,\ln 2 + \frac{4}{3}\,\zeta(2) + \frac{11}{3}\,\zeta(3)\,\ln\frac{-q^2}{\mu^2} - \frac{709}{64}\,\zeta(3)\right. \\
&\quad \left. - \frac{5}{3}\,\zeta(5) + \frac{11}{12}\,\ln\frac{-q^2}{m^2}\,\ln\frac{-q^2}{\mu^2} - \frac{71}{27}\,\ln\frac{-q^2}{m^2} - \frac{11}{24}\,\ln^2\frac{-q^2}{m^2} - \frac{539}{216}\,\ln\frac{-q^2}{\mu^2}\right) \\
&\quad + C_F\,T\,n_l\left(-\frac{295}{81} + \frac{4}{3}\,\zeta(2) - \frac{4}{3}\,\zeta(3)\,\ln\frac{-q^2}{\mu^2} + \frac{38}{9}\,\zeta(3)\right. \\
&\quad \left. - \frac{1}{3}\,\ln\frac{-q^2}{m^2}\,\ln\frac{-q^2}{\mu^2} + \frac{25}{27}\,\ln\frac{-q^2}{m^2} + \frac{1}{6}\,\ln^2\frac{-q^2}{m^2} + \frac{49}{54}\,\ln\frac{-q^2}{\mu^2}\right) \\
&\quad + C_F\,T\left(-\frac{731}{648} - \frac{8}{3}\,\zeta(2) - \frac{4}{3}\,\zeta(3)\,\ln\frac{-q^2}{\mu^2} + \frac{629}{144}\,\zeta(3)\right. \\
&\quad \left. - \frac{1}{3}\,\ln\frac{-q^2}{m^2}\,\ln\frac{-q^2}{\mu^2} + \frac{25}{27}\,\ln\frac{-q^2}{m^2} + \frac{1}{6}\,\ln^2\frac{-q^2}{m^2} + \frac{49}{54}\,\ln\frac{-q^2}{\mu^2}\right),
\end{aligned} \tag{B.5}$$

$$\begin{aligned}
D_1^{(2),a} &= C_F^2\left(\frac{111}{32} + 12\,\zeta(2)\,\ln 2\,\ln\frac{-q^2}{m^2} - 24\,\zeta(2)\,\ln 2 - \frac{15}{2}\,\zeta(2)\,\ln\frac{-q^2}{m^2} + 15\,\zeta(2)\right. \\
&\quad - \frac{15}{2}\,\zeta(3)\,\ln\frac{-q^2}{m^2} + \frac{87}{4}\,\zeta(3) - 9\,\zeta(4) - \frac{45}{2}\,\zeta(5) + \frac{3}{2}\,B_4 + \frac{127}{16}\,\ln\frac{-q^2}{m^2} \\
&\quad \left. - \frac{21}{16}\,\ln^2\frac{-q^2}{m^2} + \frac{3}{4}\,\ln^3\frac{-q^2}{m^2}\right) \\
&\quad + C_F\,C_A\left(-\frac{1219}{72} - 6\,\zeta(2)\,\ln 2\,\ln\frac{-q^2}{m^2} + 12\,\zeta(2)\,\ln 2 + 2\,\zeta(2)\,\ln\frac{-q^2}{m^2} - 4\,\zeta(2)\right. \\
&\quad - \frac{3}{4}\,\zeta(3)\,\ln\frac{-q^2}{m^2} - \frac{11}{2}\,\zeta(3)\,\ln\frac{-q^2}{\mu^2} + \frac{223}{12}\,\zeta(3) + \frac{9}{2}\,\zeta(4) - \frac{15}{4}\,\zeta(5) - \frac{3}{4}\,B_4 \\
&\quad - \frac{11}{8}\,\ln\frac{-q^2}{m^2}\,\ln\frac{-q^2}{\mu^2} + \frac{227}{48}\,\ln\frac{-q^2}{m^2} + \frac{11}{8}\,\ln^2\frac{-q^2}{m^2}\,\ln\frac{-q^2}{\mu^2} - \frac{19}{6}\,\ln^2\frac{-q^2}{m^2} \\
&\quad \left. - \frac{11}{12}\,\ln^3\frac{-q^2}{m^2} + \frac{77}{16}\,\ln\frac{-q^2}{\mu^2}\right) \\
&\quad + C_F\,T\,n_l\left(\frac{217}{36} + 2\,\zeta(2)\,\ln\frac{-q^2}{m^2} - 4\,\zeta(2) + 2\,\zeta(3)\,\ln\frac{-q^2}{\mu^2} - \frac{20}{3}\,\zeta(3)\right. \\
&\quad + \frac{1}{2}\,\ln\frac{-q^2}{m^2}\,\ln\frac{-q^2}{\mu^2} - \frac{19}{12}\,\ln\frac{-q^2}{m^2} - \frac{1}{2}\,\ln^2\frac{-q^2}{m^2}\,\ln\frac{-q^2}{\mu^2} + \frac{5}{6}\,\ln^2\frac{-q^2}{m^2} \\
&\quad \left. + \frac{1}{3}\,\ln^3\frac{-q^2}{m^2} - \frac{7}{4}\,\ln\frac{-q^2}{\mu^2}\right)
\end{aligned}$$

$$
\begin{aligned}
&+ C_F\,T\bigg(-\frac{155}{36} - 4\,\zeta(2)\,\ln\frac{-q^2}{m^2} + 8\,\zeta(2) + 2\,\zeta(3)\,\ln\frac{-q^2}{\mu^2} - \frac{23}{12}\,\zeta(3) \\
&\quad + \frac{1}{2}\,\ln\frac{-q^2}{m^2}\,\ln\frac{-q^2}{\mu^2} + \frac{17}{12}\,\ln\frac{-q^2}{m^2} - \frac{1}{2}\,\ln^2\frac{-q^2}{m^2}\,\ln\frac{-q^2}{\mu^2} + \frac{5}{6}\,\ln^2\frac{-q^2}{m^2} \\
&\quad + \frac{1}{3}\,\ln^3\frac{-q^2}{m^2} - \frac{7}{4}\,\ln\frac{-q^2}{\mu^2}\bigg), \qquad \text{(B.6)}
\end{aligned}
$$

with $\zeta(5) \approx 1.03693$. B_4 appears in our results because of the normalization condition $\Pi^a(0) = 0$.

C Analytic results for C_n^δ

In this appendix we list the first eight moments for $q^2 \to 0$ expressed in terms of the on-shell mass, m, in analytic form for the four correlators.

$$
\begin{aligned}
\Pi^{(0),v} &= \frac{3}{16\pi^2}\bigg\{\frac{16}{15}z + \frac{16}{35}z^2 + \frac{256}{945}z^3 + \frac{128}{693}z^4 + \frac{2048}{15015}z^5 + \frac{2048}{19305}z^6 + \frac{65536}{765765}z^7 \\
&\quad + \frac{16384}{230945}z^8\bigg\} + \ldots\,, \\
\Pi^{(1),v} &= \frac{3}{16\pi^2}\bigg\{\frac{328}{81}z + \frac{1796}{675}z^2 + \frac{999664}{496125}z^3 + \frac{207944}{127575}z^4 + \frac{1729540864}{1260653625}z^5 \\
&\quad + \frac{21660988864}{18261468225}z^6 + \frac{401009026048}{383490832725}z^7 + \frac{633021048064}{676610809875}z^8\bigg\} + \ldots\,, \\
C_1^{(2),v} &= C_F^2\bigg(-\frac{8687}{864} - \frac{32}{5}\,\zeta(2)\,\ln 2 + 4\,\zeta(2) + \frac{22781}{1728}\,\zeta(3)\bigg) \\
&\quad + C_F\,C_A\bigg(\frac{127}{192} + \frac{902}{243}\,\ln\frac{\mu^2}{m^2} + \frac{16}{5}\,\zeta(2)\,\ln 2 - \frac{16}{15}\,\zeta(2) + \frac{1451}{384}\,\zeta(3)\bigg) \\
&\quad + C_F\,T\,n_l\bigg(-\frac{142}{243} - \frac{328}{243}\,\ln\frac{\mu^2}{m^2} - \frac{16}{15}\,\zeta(2)\bigg) \\
&\quad + C_F\,T\bigg(-\frac{11407}{2916} - \frac{328}{243}\,\ln\frac{\mu^2}{m^2} + \frac{32}{15}\,\zeta(2) + \frac{203}{216}\,\zeta(3)\bigg), \\
C_2^{(2),v} &= C_F^2\bigg(-\frac{223404289}{1866240} - \frac{192}{35}\,\zeta(2)\,\ln 2 + \frac{24}{7}\,\zeta(2) + \frac{4857587}{46080}\,\zeta(3)\bigg) \\
&\quad + C_F\,C_A\bigg(-\frac{1030213543}{93312000} + \frac{4939}{2025}\,\ln\frac{\mu^2}{m^2} + \frac{96}{35}\,\zeta(2)\,\ln 2 - \frac{32}{35}\,\zeta(2) \\
&\quad + \frac{723515}{55296}\,\zeta(3)\bigg) + C_F\,T\,n_l\bigg(-\frac{40703}{60750} - \frac{1796}{2025}\,\ln\frac{\mu^2}{m^2} - \frac{32}{35}\,\zeta(2)\bigg) \\
&\quad + C_F\,T\bigg(-\frac{1520789}{414720} - \frac{1796}{2025}\,\ln\frac{\mu^2}{m^2} + \frac{64}{35}\,\zeta(2) + \frac{14203}{18432}\,\zeta(3)\bigg),
\end{aligned}
$$

$$
\begin{aligned}
C_3^{(2),v} &= C_F^2 \left(-\frac{885937890461}{1161216000} - \frac{512}{105}\zeta(2)\,\ln 2 + \frac{64}{21}\zeta(2) + \frac{33067024499}{51609600}\zeta(3) \right) \\
&+ C_F\,C_A \left(-\frac{95905830011197}{1706987520000} + \frac{2749076}{1488375}\,\ln\frac{\mu^2}{m^2} + \frac{256}{105}\zeta(2)\,\ln 2 \right. \\
&\left. - \frac{256}{315}\zeta(2) + \frac{5164056461}{103219200}\zeta(3) \right) \\
&+ C_F\,T\,n_l \left(-\frac{9703588}{17364375} - \frac{999664}{1488375}\,\ln\frac{\mu^2}{m^2} - \frac{256}{315}\zeta(2) \right) \\
&+ C_F\,T \left(-\frac{83936527}{23328000} - \frac{999664}{1488375}\,\ln\frac{\mu^2}{m^2} + \frac{512}{315}\zeta(2) + \frac{12355}{13824}\zeta(3) \right), \\
C_4^{(2),v} &= C_F^2 \left(-\frac{2692406698848 18833}{61451550720000} - \frac{1024}{231}\zeta(2)\,\ln 2 + \frac{640}{231}\zeta(2) \right. \\
&\left. + \frac{1507351507033}{412876800}\zeta(3) \right) + C_F\,C_A \left(-\frac{36675392331131681}{158018273280000} + \frac{571846}{382725}\,\ln\frac{\mu^2}{m^2} \right. \\
&\left. + \frac{512}{231}\zeta(2)\,\ln 2 - \frac{512}{693}\zeta(2) + \frac{1455887207647}{7431782400}\zeta(3) \right) \\
&+ C_F\,T\,n_l \left(-\frac{54924808}{120558375} - \frac{207944}{382725}\,\ln\frac{\mu^2}{m^2} - \frac{512}{693}\zeta(2) \right) \\
&+ C_F\,T \left(-\frac{129586264289}{35831808000} - \frac{207944}{382725}\,\ln\frac{\mu^2}{m^2} + \frac{1024}{693}\zeta(2) + \frac{2522821}{2359296}\zeta(3) \right), \\
C_5^{(2),v} &= C_F^2 \left(-\frac{360248170450504167133}{15209258803200000} - \frac{4096}{1001}\zeta(2)\,\ln 2 + \frac{2560}{1001}\zeta(2) \right. \\
&\left. + \frac{939939943788973}{47687270400}\zeta(3) \right) + C_F\,C_A \left(-\frac{21883348499544169357}{23658847027200000} \right. \\
&\left. + \frac{432385216}{343814625}\,\ln\frac{\mu^2}{m^2} + \frac{2048}{1001}\zeta(2)\,\ln 2 - \frac{2048}{3003}\zeta(2) + \frac{14724562345079}{19074908160}\zeta(3) \right) \\
&+ C_F\,T\,n_l \left(-\frac{4881989801536}{13104494431875} - \frac{1729540864}{3781960875}\,\ln\frac{\mu^2}{m^2} - \frac{2048}{3003}\zeta(2) \right) \\
&+ C_F\,T \left(-\frac{512847330943}{139087872000} - \frac{1729540864}{3781960875}\,\ln\frac{\mu^2}{m^2} \right. \\
&\left. + \frac{4096}{3003}\zeta(2) + \frac{1239683}{983040}\zeta(3) \right), \\
C_6^{(2),v} &= C_F^2 \left(-\frac{64959156551995419148501103}{529285210649395200000} - \frac{8192}{2145}\zeta(2)\,\ln 2 + \frac{1024}{429}\zeta(2) \right. \\
&\left. + \frac{330704075360938001}{3238841548800}\zeta(3) \right)
\end{aligned}
$$

$$
\begin{aligned}
&+ C_F\,C_A \left(- \frac{4826864658245605658856745531}{1317342772469012889600000} + \frac{5415247216}{4980400425}\,\ln\frac{\mu^2}{m^2} \right.\\
&\left. + \frac{4096}{2145}\,\zeta(2)\,\ln 2 - \frac{4096}{6435}\,\zeta(2) + \frac{580922571682067161}{190443883069440}\,\zeta(3) \right)\\
&+ C_F\,T\,n_l \left(- \frac{151249070952032}{493552701717075} - \frac{21660988864}{54784404675}\,\ln\frac{\mu^2}{m^2} - \frac{4096}{6435}\,\zeta(2) \right)\\
&+ C_F\,T \left(- \frac{3411069430668887863}{899847347503104000} - \frac{21660988864}{54784404675}\,\ln\frac{\mu^2}{m^2} \right.\\
&\left. + \frac{8192}{6435}\,\zeta(2) + \frac{1760922667}{1207959552}\,\zeta(3) \right),\\
C_7^{(2),v} &= C_F^2 \left(- \frac{57136589735109062714804541392 3471}{92740931181818507427840000 0} - \frac{131072}{36465}\,\zeta(2)\,\ln 2 \right.\\
&\left. + \frac{16384}{7293}\,\zeta(2) + \frac{13386367971827490465799}{26118018249523200}\,\zeta(3) \right)\\
&+ C_F\,C_A \left(- \frac{7342721436809271685822267340249}{50585962462810094960640000 0} + \frac{100252256512}{104588408925}\,\ln\frac{\mu^2}{m^2} \right.\\
&\left. + \frac{65536}{36465}\,\zeta(2)\,\ln 2 - \frac{65536}{109395}\,\zeta(2) + \frac{14019414333929589373}{1160800811089920}\,\zeta(3) \right)\\
&+ C_F\,T\,n_l \left(- \frac{13125091764358528}{51823033680292875} - \frac{401009026048}{1150472498175}\,\ln\frac{\mu^2}{m^2} - \frac{65536}{109395}\,\zeta(2) \right)\\
&+ C_F\,T \left(- \frac{7927736038867601807}{2024656531881984000} - \frac{401009026048}{1150472498175}\,\ln\frac{\mu^2}{m^2} \right.\\
&\left. + \frac{131072}{109395}\,\zeta(2) + \frac{4497899939}{2717908992}\,\zeta(3) \right),\\
C_8^{(2),v} &= C_F^2 \left(- \frac{19030218241725531289888611 5648452691}{63063833203636585050931200000} \right.\\
&\left. - \frac{786432}{230945}\,\zeta(2)\,\ln 2 + \frac{98304}{46189}\,\zeta(2) + \frac{31209476560803609727258477}{12432176686773043200}\,\zeta(3) \right)\\
&+ C_F\,C_A \left(- \frac{1141319692437947188024886706606 5741}{19825661937988626504744960000 0} + \frac{393216}{230945}\,\zeta(2)\,\ln 2 \right.\\
&\left. - \frac{131072}{230945}\,\zeta(2) + \frac{2430254187345828028006 7}{507435783133593600}\,\zeta(3) + \frac{158255262016}{184530220875}\,\ln\frac{\mu^2}{m^2} \right)\\
&+ C_F\,T\,n_l \left(- \frac{65233327834094144}{310874926094357625} - \frac{633021048064}{2029832429625}\,\ln\frac{\mu^2}{m^2} - \frac{131072}{230945}\,\zeta(2) \right)\\
&+ C_F\,T \left(- \frac{23818697864446985668391}{5874203484500262912000} - \frac{633021048064}{2029832429625}\,\ln\frac{\mu^2}{m^2} \right.
\end{aligned}
$$

$$+\frac{262144}{230945}\,\zeta(2)+\frac{286122897977}{154618822656}\,\zeta(3)\Big), \qquad \text{(C.1)}$$

$$\begin{aligned}
\Pi^{(0),a} &= \frac{3}{16\pi^2}\Big\{\frac{8}{15}z+\frac{16}{105}z^2+\frac{64}{945}z^3+\frac{128}{3465}z^4+\frac{1024}{45045}z^5+\frac{2048}{135135}z^6+\frac{8192}{765765}z^7 \\
&\quad +\frac{16384}{2078505}z^8\Big\}+\ldots\ , \\
\Pi^{(1),a} &= \frac{3}{16\pi^2}\Big\{\frac{689}{405}z+\frac{3382}{4725}z^2+\frac{196852}{496125}z^3+\frac{12398216}{49116375}z^4+\frac{318252608}{1820944125}z^5 \\
&\quad +\frac{655479040}{5113211103}z^6+\frac{639246915968}{6519344156325}z^7+\frac{38821601949952}{501368610117375}z^8\Big\}+\ldots\ , \\
C_1^{(2),a} &= C_F^2\left(\frac{2237369}{51840}-\frac{16}{5}\,\zeta(2)\,\ln 2+2\,\zeta(2)-\frac{1164013}{34560}\,\zeta(3)\right) \\
&\quad + C_F\,C_A\left(\frac{3226373}{311040}+\frac{8}{5}\,\zeta(2)\,\ln 2-\frac{8}{15}\,\zeta(2)-\frac{494867}{69120}\,\zeta(3)+\frac{7579}{4860}\,\ln\frac{\mu^2}{m^2}\right) \\
&\quad + C_F\,T\,n_l\left(-\frac{137}{810}-\frac{8}{15}\,\zeta(2)-\frac{689}{1215}\,\ln\frac{\mu^2}{m^2}\right) \\
&\quad + C_F\,T\left(-\frac{433669}{186624}+\frac{16}{15}\,\zeta(2)+\frac{10493}{13824}\,\zeta(3)-\frac{689}{1215}\,\ln\frac{\mu^2}{m^2}\right), \\
C_2^{(2),a} &= C_F^2\left(\frac{7672813249}{26127360}-\frac{64}{35}\,\zeta(2)\,\ln 2+\frac{8}{7}\,\zeta(2)-\frac{2349181181}{9676800}\,\zeta(3)\right) \\
&\quad + C_F\,C_A\left(\frac{47328042151}{1306368000}+\frac{32}{35}\,\zeta(2)\,\ln 2-\frac{32}{105}\,\zeta(2)-\frac{188251393}{6451200}\,\zeta(3)\right. \\
&\quad \left.+\frac{18601}{28350}\,\ln\frac{\mu^2}{m^2}\right)+C_F\,T\,n_l\left(-\frac{1097}{6750}-\frac{32}{105}\,\zeta(2)-\frac{3382}{14175}\,\ln\frac{\mu^2}{m^2}\right) \\
&\quad + C_F\,T\left(-\frac{27450553}{17418240}+\frac{64}{105}\,\zeta(2)+\frac{19579}{36864}\,\zeta(3)-\frac{3382}{14175}\,\ln\frac{\mu^2}{m^2}\right), \\
C_3^{(2),a} &= C_F^2\left(\frac{111399585201971}{58525286400}-\frac{128}{105}\,\zeta(2)\,\ln 2+\frac{16}{21}\,\zeta(2)-\frac{979995241517}{619315200}\,\zeta(3)\right) \\
&\quad + C_F\,C_A\left(\frac{2930267790199843}{20483850240000}+\frac{64}{105}\,\zeta(2)\,\ln 2-\frac{64}{315}\,\zeta(2)\right. \\
&\quad \left.-\frac{146653533139}{1238630400}\,\zeta(3)+\frac{541343}{1488375}\,\ln\frac{\mu^2}{m^2}\right) \\
&\quad + C_F\,T\,n_l\left(-\frac{5058122}{52093125}-\frac{64}{315}\,\zeta(2)-\frac{196852}{1488375}\,\ln\frac{\mu^2}{m^2}\right) \\
&\quad + C_F\,T\left(-\frac{26031430073}{20901888000}+\frac{128}{315}\,\zeta(2)+\frac{4411519}{8847360}\,\zeta(3)-\frac{196852}{1488375}\,\ln\frac{\mu^2}{m^2}\right),
\end{aligned}$$

$$
\begin{aligned}
C_4^{(2),a} &= C_F^2 \left(\frac{308356223383353917}{27590492160000} - \frac{1024}{1155}\,\zeta(2)\,\ln 2 + \frac{128}{231}\,\zeta(2) \right. \\
&\left. - \frac{197037714570097}{21194342400}\,\zeta(3) \right) + C_F\,C_A \left(\frac{1275464959378469537}{2212255825920000} \right. \\
&\left. + \frac{512}{1155}\,\zeta(2)\,\ln 2 - \frac{512}{3465}\,\zeta(2) - \frac{109692872248273}{228898897920}\,\zeta(3) + \frac{3099554}{13395375}\,\ln\frac{\mu^2}{m^2} \right) \\
&+ C_F\,T\,n_l \left(-\frac{2710286584}{46414974375} - \frac{512}{3465}\,\zeta(2) - \frac{12398216}{147349125}\,\ln\frac{\mu^2}{m^2} \right) \\
&+ C_F\,T \left(-\frac{731128794367}{689762304000} + \frac{1024}{3465}\,\zeta(2) + \frac{1432739}{2949120}\,\zeta(3) - \frac{12398216}{147349125}\,\ln\frac{\mu^2}{m^2} \right), \\
C_5^{(2),a} &= C_F^2 \left(\frac{42770055318320138453900 21}{69597568283443200000} - \frac{2048}{3003}\,\zeta(2)\,\ln 2 \right. \\
&\left. + \frac{1280}{3003}\,\zeta(2) - \frac{10141704975198352 31}{19837904486400}\,\zeta(3) \right) \\
&+ C_F\,C_A \left(\frac{581194529682893414245 39}{249837424607232000 00} + \frac{1024}{3003}\,\zeta(2)\,\ln 2 \right. \\
&\left. - \frac{1024}{9009}\,\zeta(2) - \frac{2193462351270763}{1133594542080}\,\zeta(3) + \frac{79563152}{496621125}\,\ln\frac{\mu^2}{m^2} \right) \\
&+ C_F\,T\,n_l \left(-\frac{226047457424}{6309571393125} - \frac{1024}{9009}\,\zeta(2) - \frac{318252608}{5462832375}\,\ln\frac{\mu^2}{m^2} \right) \\
&+ C_F\,T \left(-\frac{5461272114191}{5796790272000} + \frac{2048}{9009}\,\zeta(2) + \frac{30020447}{62914560}\,\zeta(3) \right. \\
&\left. - \frac{318252608}{5462832375}\,\ln\frac{\mu^2}{m^2} \right), \\
C_6^{(2),a} &= C_F^2 \left(\frac{35974544881029356271640023 0493}{11146746536276262912000 00} - \frac{8192}{15015}\,\zeta(2)\,\ln 2 \right. \\
&\left. + \frac{1024}{3003}\,\zeta(2) - \frac{232415799530843949 19}{86565401395200}\,\zeta(3) \right) \\
&+ C_F\,C_A \left(\frac{246947968076301121046020861 97}{26346855449380257792000 00} + \frac{4096}{15015}\,\zeta(2)\,\ln 2 \right. \\
&\left. - \frac{4096}{45045}\,\zeta(2) - \frac{761503054628786 41}{9766352977920}\,\zeta(3) + \frac{163869760}{1394512119}\,\ln\frac{\mu^2}{m^2} \right) \\
&+ C_F\,T\,n_l \left(-\frac{381648296450416}{17274344560097625} - \frac{4096}{45045}\,\zeta(2) - \frac{655479040}{15339633309}\,\ln\frac{\mu^2}{m^2} \right) \\
&+ C_F\,T \left(-\frac{15488259621125158 19}{17996946950062080 00} + \frac{8192}{45045}\,\zeta(2) \right.
\end{aligned}
$$

$$
\begin{aligned}
&+ \frac{1134854351}{2415919104}\,\zeta(3) - \frac{655479040}{15339633309}\,\ln\frac{\mu^2}{m^2}\Bigg),\\
C_7^{(2),a} &= C_F^2\left(\frac{22958500659171861410747168121336 31}{14014185156363685566873600 00} - \frac{16384}{36465}\,\zeta(2)\,\ln 2\right.\\
&\left. + \frac{2048}{7293}\,\zeta(2) - \frac{24204696321513923806403 63}{1776025240967577600}\,\zeta(3)\right)\\
&+ C_F\,C_A\left(\frac{11792676410737277924078160740 7103}{31271322249737149612032000 00} + \frac{8192}{36465}\,\zeta(2)\,\ln 2\right.\\
&\left. - \frac{8192}{109395}\,\zeta(2) - \frac{11143403181401225390581 3}{3552050481935155200}\,\zeta(3) + \frac{159811728992}{1778002951725}\,\ln\frac{\mu^2}{m^2}\right)\\
&+ C_F\,T\,n_l\left(-\frac{2357049928630816}{176198314512995775} - \frac{8192}{109395}\,\zeta(2)\right.\\
&\left. - \frac{639246915968}{19558032468975}\,\ln\frac{\mu^2}{m^2}\right) + C_F\,T\left(-\frac{7054922290825747665 43}{8811305226750394368 00}\right.\\
&\left. + \frac{16384}{109395}\,\zeta(2) + \frac{161018056831}{347892350976}\,\zeta(3) - \frac{639246915968}{19558032468975}\,\ln\frac{\mu^2}{m^2}\right),\\
C_8^{(2),a} &= C_F^2\left(\frac{36666382863813217294681656413671975999}{45265818055054704381001728 00000} - \frac{262144}{692835}\,\zeta(2)\,\ln 2\right.\\
&\left. + \frac{32768}{138567}\,\zeta(2) - \frac{38909315504947373771077216 91}{577405539452348006400}\,\zeta(3)\right)\\
&+ C_F\,C_A\left(\frac{48981533459508434778776522917210636 5989}{32319794091309058928035233792000 00} + \frac{131072}{692835}\,\zeta(2)\,\ln 2\right.\\
&\left. - \frac{131072}{2078505}\,\zeta(2) - \frac{52435508642065686120 3887}{4158983477447884800}\,\zeta(3)\right.\\
&\left. + \frac{9705400487488}{136736893668375}\,\ln\frac{\mu^2}{m^2}\right)\\
&+ C_F\,T\,n_l\left(-\frac{17622323865355692 16}{230358320235919000125} - \frac{131072}{2078505}\,\zeta(2)\right.\\
&\left. - \frac{38821601949952}{1504105830352125}\,\ln\frac{\mu^2}{m^2}\right) + C_F\,T\left(-\frac{84212007346306764915559}{11160986620550499532800 0}\right.\\
&\left. + \frac{262144}{2078505}\,\zeta(2) + \frac{1058200490221}{2319282339840}\,\zeta(3) - \frac{38821601949952}{1504105830352125}\,\ln\frac{\mu^2}{m^2}\right), \qquad \text{(C.2)}
\end{aligned}
$$

$$
\begin{aligned}
\Pi^{(0),s} &= \frac{3}{16\pi^2}\left\{\frac{4}{5}z + \frac{8}{35}z^2 + \frac{32}{315}z^3 + \frac{64}{1155}z^4 + \frac{512}{15015}z^5 + \frac{1024}{45045}z^6 + \frac{4096}{255255}z^7\right.\\
&\left. + \frac{8192}{692835}z^8\right\} + \ldots\ ,
\end{aligned}
$$

$$
\begin{aligned}
\Pi^{(1),s} &= \frac{3}{16\pi^2}\Big\{\frac{61}{135}z + \frac{1223}{1575}z^2 + \frac{86246}{165375}z^3 + \frac{5845948}{16372125}z^4 + \frac{155689024}{606981375}z^5 \\
&\quad + \frac{1637544448}{8522018505}z^6 + \frac{323629508032}{2173114718775}z^7 + \frac{19824721740416}{167122870039125}z^8\Big\} + \ldots \;, \\
C_1^{(2),s} &= C_F^2\left(\frac{413}{30} - \frac{1645}{144}\,\zeta(3)\right) + C_F\,C_A\left(-\frac{191}{648} - \frac{59}{32}\,\zeta(3) + \frac{671}{1620}\,\ln\frac{\mu^2}{m^2}\right) \\
&\quad + C_F\,T\,n_l\left(\frac{119}{135} - \frac{61}{405}\,\ln\frac{\mu^2}{m^2}\right) + C_F\,T\left(-\frac{60559}{77760} + \frac{1435}{1152}\,\zeta(3) - \frac{61}{405}\,\ln\frac{\mu^2}{m^2}\right), \\
C_2^{(2),s} &= C_F^2\left(\frac{627541597}{10886400} - \frac{48}{35}\,\zeta(2)\,\ln 2 + \frac{6}{7}\,\zeta(2) - \frac{1074607}{23040}\,\zeta(3)\right) \\
&\quad + C_F\,C_A\left(+\frac{991366223}{108864000} + \frac{24}{35}\,\zeta(2)\,\ln 2 - \frac{8}{35}\,\zeta(2) - \frac{110107}{15360}\,\zeta(3)\right. \\
&\quad \left. + \frac{13453}{18900}\,\ln\frac{\mu^2}{m^2}\right) + C_F\,T\,n_l\left(+\frac{797}{47250} - \frac{8}{35}\,\zeta(2) - \frac{1223}{4725}\,\ln\frac{\mu^2}{m^2}\right) \\
&\quad + C_F\,T\left(-\frac{1685773}{1161216} + \frac{16}{35}\,\zeta(2) + \frac{9107}{12288}\,\zeta(3) - \frac{1223}{4725}\,\ln\frac{\mu^2}{m^2}\right), \\
C_3^{(2),s} &= C_F^2\left(\frac{1619371436071}{4064256000} - \frac{128}{105}\,\zeta(2)\,\ln 2 + \frac{16}{21}\,\zeta(2) - \frac{405607027}{1228800}\,\zeta(3)\right) \\
&\quad + C_F\,C_A\left(\frac{11448730350251}{284497920000} + \frac{64}{105}\,\zeta(2)\,\ln 2 - \frac{64}{315}\,\zeta(2) - \frac{566787803}{17203200}\,\zeta(3)\right. \\
&\quad \left. + \frac{474353}{992250}\,\ln\frac{\mu^2}{m^2}\right) + C_F\,T\,n_l\left(-\frac{1146421}{17364375} - \frac{64}{315}\,\zeta(2) - \frac{86246}{496125}\,\ln\frac{\mu^2}{m^2}\right) \\
&\quad + C_F\,T\left(-\frac{694040519}{497664000} + \frac{128}{315}\,\zeta(2) + \frac{978439}{1474560}\,\zeta(3) - \frac{86246}{496125}\,\ln\frac{\mu^2}{m^2}\right), \\
C_4^{(2),s} &= C_F^2\left(\frac{147161013073070141}{56330588160000} - \frac{384}{385}\,\zeta(2)\,\ln 2 + \frac{48}{77}\,\zeta(2)\right. \\
&\quad \left. - \frac{224204681453}{103219200}\,\zeta(3)\right) + C_F\,C_A\left(\frac{35969257153127519}{202790117376000} + \frac{192}{385}\,\zeta(2)\,\ln 2\right. \\
&\quad \left. - \frac{64}{385}\,\zeta(2) - \frac{18221998757}{123863040}\,\zeta(3) + \frac{1461487}{4465125}\,\ln\frac{\mu^2}{m^2}\right) \\
&\quad + C_F\,T\,n_l\left(-\frac{930573962}{15471658125} - \frac{64}{385}\,\zeta(2) - \frac{5845948}{49116375}\,\ln\frac{\mu^2}{m^2}\right) \\
&\quad + C_F\,T\left(-\frac{590888856583}{459841536000} + \frac{128}{385}\,\zeta(2) + \frac{1262219}{1966080}\,\zeta(3) - \frac{5845948}{49116375}\,\ln\frac{\mu^2}{m^2}\right), \\
C_5^{(2),s} &= C_F^2\left(\frac{45884811924398978440541}{28998986784768000000} - \frac{4096}{5005}\,\zeta(2)\,\ln 2 + \frac{512}{1001}\,\zeta(2)\right.
\end{aligned}
$$

$$
\begin{aligned}
&- \frac{13283992935869}{1009254400}\,\zeta(3)\Bigg) + C_F\,C_A\,\Bigg(\frac{945084080119306598357}{1230260045414400000}\\
&+ \frac{2048}{5005}\,\zeta(2)\,\ln 2 - \frac{2048}{15015}\,\zeta(2) - \frac{5414889135283}{8477736960}\,\zeta(3) + \frac{38922256}{165540375}\,\ln\frac{\mu^2}{m^2}\Bigg)\\
&+ C_F\,T\,n_l\,\Bigg(-\frac{21726270352}{485351645625} - \frac{2048}{15015}\,\zeta(2) - \frac{155689024}{1820944125}\,\ln\frac{\mu^2}{m^2}\Bigg)\\
&+ C_F\,T\,\Bigg(-\frac{413776570931}{347163328512} + \frac{4096}{15015}\,\zeta(2) + \frac{1660607}{2621440}\,\zeta(3)\\
&- \frac{155689024}{1820944125}\,\ln\frac{\mu^2}{m^2}\Bigg),\\
C_6^{(2),s} &= C_F^2\,\Bigg(\frac{39750173166315234163298379 1}{4423312117569945600000} - \frac{2048}{3003}\,\zeta(2)\,\ln 2 + \frac{1280}{3003}\,\zeta(2)\\
&- \frac{1977406903785590041}{26450539315200}\,\zeta(3)\Bigg) + C_F\,C_A\,\Bigg(\frac{71752237844000299550029337 9}{219557128744835481600000}\\
&+ \frac{1024}{3003}\,\zeta(2)\,\ln 2 - \frac{1024}{9009}\,\zeta(2) - \frac{12326391884997959}{4534378168320}\,\zeta(3)\\
&+ \frac{409386112}{2324186865}\,\ln\frac{\mu^2}{m^2}\Bigg) + C_F\,T\,n_l\,\Bigg(-\frac{7250780973536}{230324594134635} - \frac{1024}{9009}\,\zeta(2)\\
&- \frac{1637544448}{25566055515}\,\ln\frac{\mu^2}{m^2}\Bigg) + C_F\,T\,\Bigg(-\frac{51604525307586967}{46146017820672000} + \frac{2048}{9009}\,\zeta(2)\\
&+ \frac{506059663}{805306368}\,\zeta(3) - \frac{1637544448}{25566055515}\,\ln\frac{\mu^2}{m^2}\Bigg),\\
C_7^{(2),s} &= C_F^2\,\Bigg(\frac{27815080684623961206688370396051}{57247488838383858483200000} - \frac{49152}{85085}\,\zeta(2)\,\ln 2\\
&+ \frac{6144}{17017}\,\zeta(2) - \frac{1599537316283284324 43}{395727549235200}\,\zeta(3)\Bigg)\\
&+ C_F\,C_A\,\Bigg(\frac{19658778113043866943074074991111}{14332689364462860238848000 00} + \frac{24576}{85085}\,\zeta(2)\,\ln 2\\
&- \frac{8192}{85085}\,\zeta(2) - \frac{2207504939742233011}{193466801848320}\,\zeta(3) + \frac{80907377008}{592667650575}\,\ln\frac{\mu^2}{m^2}\Bigg)\\
&+ C_F\,T\,n_l\,\Bigg(-\frac{6298337396620816}{293663857521659625} - \frac{8192}{85085}\,\zeta(2) - \frac{323629508032}{6519344156325}\,\ln\frac{\mu^2}{m^2}\Bigg)\\
&+ C_F\,T\,\Bigg(-\frac{111176247094824256811}{1048964907946475520 00} + \frac{16384}{85085}\,\zeta(2)\\
&+ \frac{36189456601}{57982058496}\,\zeta(3) - \frac{323629508032}{6519344156325}\,\ln\frac{\mu^2}{m^2}\Bigg),
\end{aligned}
$$

$$
\begin{aligned}
C_8^{(2),s} &= C_F^2 \left(\frac{90860323801590559420949997562702411}{35925252424646590778572800000} - \frac{114688}{230945}\,\zeta(2)\,\ln 2 \right. \\
&\left. + \frac{14336}{46189}\,\zeta(2) - \frac{87191714446859913989310 83}{4144058895591014400}\,\zeta(3) \right) \\
&+ C_F\,C_A \left(\frac{27914913856435723062167953570837683 11}{48969384986831907466720051200000} + \frac{57344}{230945}\,\zeta(2)\,\ln 2 \right. \\
&\left. - \frac{57344}{692835}\,\zeta(2) - \frac{8912555608537907321 89}{18793917893836800}\,\zeta(3) + \frac{4956180435104}{45578964556125}\,\ln\frac{\mu^2}{m^2} \right) \\
&+ C_F\,T\,n_l \left(-\frac{216441517065785056}{15357221349061266675} - \frac{57344}{692835}\,\zeta(2) \right. \\
&\left. - \frac{19824721740416}{501368610117375}\,\ln\frac{\mu^2}{m^2} \right) + C_F\,T \left(-\frac{75342677076574228286 83}{74406577470336663552 00} \right. \\
&\left. + \frac{114688}{692835}\,\zeta(2) + \frac{479255846237}{773094113280}\,\zeta(3) - \frac{19824721740416}{501368610117375}\,\ln\frac{\mu^2}{m^2} \right), \qquad \text{(C.3)}
\end{aligned}
$$

$$
\begin{aligned}
\Pi^{(0),p} &= \frac{3}{16\pi^2}\left\{ \frac{4}{3}z + \frac{8}{15}z^2 + \frac{32}{105}z^3 + \frac{64}{315}z^4 + \frac{512}{3465}z^5 + \frac{1024}{9009}z^6 + \frac{4096}{45045}z^7 \right. \\
&\left. + \frac{8192}{109395}z^8 \right\} + \dots\ , \\
\Pi^{(1),p} &= \frac{3}{16\pi^2}\left\{ \frac{7}{3}z + \frac{353}{135}z^2 + \frac{10054}{4725}z^3 + \frac{96668}{55125}z^4 + \frac{24281408}{16372125}z^5 \right. \\
&\left. + \frac{4203369152}{3277699425}z^6 + \frac{1781242688}{1578151575}z^7 + \frac{312784060544}{310444959825}z^8 \right\} + \dots\ , \\
C_1^{(2),p} &= C_F^2 \left(-\frac{401}{144} + \frac{439}{96}\,\zeta(3) \right) + C_F\,C_A \left(-\frac{3385}{864} + \frac{329}{192}\,\zeta(3) + \frac{77}{36}\,\ln\frac{\mu^2}{m^2} \right) \\
&+ C_F\,T\,n_l \left(\frac{25}{27} - \frac{7}{9}\,\ln\frac{\mu^2}{m^2} \right) + C_F\,T \left(\frac{7}{27} + \frac{7}{8}\,\zeta(3) - \frac{7}{9}\,\ln\frac{\mu^2}{m^2} \right), \\
C_2^{(2),p} &= C_F^2 \left(-\frac{1100707}{17280} - \frac{16}{5}\,\zeta(2)\,\ln 2 + 2\,\zeta(2) + \frac{681359}{11520}\,\zeta(3) \right) \\
&+ C_F\,C_A \left(-\frac{1137479}{103680} + \frac{8}{5}\,\zeta(2)\,\ln 2 - \frac{8}{15}\,\zeta(2) + \frac{28969}{2560}\,\zeta(3) + \frac{3883}{1620}\,\ln\frac{\mu^2}{m^2} \right) \\
&+ C_F\,T\,n_l \left(-\frac{287}{810} - \frac{8}{15}\,\zeta(2) - \frac{353}{405}\,\ln\frac{\mu^2}{m^2} \right) \\
&+ C_F\,T \left(-\frac{98605}{62208} + \frac{16}{15}\,\zeta(2) + \frac{1253}{4608}\,\zeta(3) - \frac{353}{405}\,\ln\frac{\mu^2}{m^2} \right), \\
C_3^{(2),p} &= C_F^2 \left(-\frac{22191983083}{43545600} - \frac{128}{35}\,\zeta(2)\,\ln 2 + \frac{16}{7}\,\zeta(2) + \frac{1390832179}{3225600}\,\zeta(3) \right)
\end{aligned}
$$

$$
\begin{aligned}
&+ C_F\,C_A \left(-\frac{4990621717}{87091200} + \frac{64}{35}\,\zeta(2)\,\ln 2 - \frac{64}{105}\,\zeta(2) + \frac{107917807}{2150400}\,\zeta(3) \right. \\
&\left. + \frac{55297}{28350}\,\ln\frac{\mu^2}{m^2} \right) + C_F\,T\,n_l \left(-\frac{1687}{3375} - \frac{64}{105}\,\zeta(2) - \frac{10054}{14175}\,\ln\frac{\mu^2}{m^2} \right) \\
&+ C_F\,T \left(-\frac{36123823}{17418240} + \frac{128}{105}\,\zeta(2) + \frac{10045}{36864}\,\zeta(3) - \frac{10054}{14175}\,\ln\frac{\mu^2}{m^2} \right), \\
C_4^{(2),p} &= C_F^2 \left(-\frac{329691878962513}{97542144000} - \frac{128}{35}\,\zeta(2)\,\ln 2 + \frac{16}{7}\,\zeta(2) + \frac{581996570819}{206438400}\,\zeta(3) \right) \\
&+ C_F\,C_A \left(-\frac{571511627867983}{2275983360000} + \frac{64}{35}\,\zeta(2)\,\ln 2 - \frac{64}{105}\,\zeta(2) \right. \\
&\left. + \frac{17445959641}{82575360}\,\zeta(3) + \frac{265837}{165375}\,\ln\frac{\mu^2}{m^2} \right) \\
&+ C_F\,T\,n_l \left(-\frac{8198894}{17364375} - \frac{64}{105}\,\zeta(2) - \frac{96668}{165375}\,\ln\frac{\mu^2}{m^2} \right) \\
&+ C_F\,T \left(-\frac{1077978107}{464486400} + \frac{128}{105}\,\zeta(2) + \frac{130123}{327680}\,\zeta(3) - \frac{96668}{165375}\,\ln\frac{\mu^2}{m^2} \right), \\
C_5^{(2),p} &= C_F^2 \left(-\frac{9089416219983580783}{450644705280000} - \frac{4096}{1155}\,\zeta(2)\,\ln 2 + \frac{512}{231}\,\zeta(2) \right. \\
&\left. + \frac{213469483642711}{12716605440}\,\zeta(3) \right) + C_F\,C_A \left(-\frac{771845002398293227}{737418608640000} \right. \\
&\left. + \frac{2048}{1155}\,\zeta(2)\,\ln 2 - \frac{2048}{3465}\,\zeta(2) + \frac{66603161317883}{76299632640}\,\zeta(3) + \frac{6070352}{4465125}\,\ln\frac{\mu^2}{m^2} \right) \\
&+ C_F\,T\,n_l \left(-\frac{6409976752}{15471658125} - \frac{2048}{3465}\,\zeta(2) - \frac{24281408}{49116375}\,\ln\frac{\mu^2}{m^2} \right) \\
&+ C_F\,T \left(-\frac{329953898617}{131383296000} + \frac{4096}{3465}\,\zeta(2) + \frac{2222003}{3932160}\,\zeta(3) \right. \\
&\left. - \frac{24281408}{49116375}\,\ln\frac{\mu^2}{m^2} \right), \\
C_6^{(2),p} &= C_F^2 \left(-\frac{372359772998064628281949}{3314169918259200000} - \frac{10240}{3003}\,\zeta(2)\,\ln 2 + \frac{6400}{3003}\,\zeta(2) \right. \\
&\left. + \frac{618116373887820433}{6612634828800}\,\zeta(3) \right) + C_F\,C_A \left(-\frac{1072111616262230016648 31}{249837424607232000 00} \right. \\
&\left. + \frac{5120}{3003}\,\zeta(2)\,\ln 2 - \frac{5120}{9009}\,\zeta(2) + \frac{115687685688677}{32388415488}\,\zeta(3) + \frac{1050842288}{893918025}\,\ln\frac{\mu^2}{m^2} \right) \\
&+ C_F\,T\,n_l \left(-\frac{12132112100624}{34071685522875} - \frac{5120}{9009}\,\zeta(2) \right.
\end{aligned}
$$

$$
\begin{aligned}
&- \frac{4203369152}{9833098275}\,\ln\frac{\mu^2}{m^2}\Big) + C_F\,T\,\Big(- \frac{2290986762786311}{852128169984000} + \frac{10240}{9009}\,\zeta(2)\\
&+ \frac{9445897}{12582912}\,\zeta(3) - \frac{4203369152}{9833098275}\,\ln\frac{\mu^2}{m^2}\Big),\\
C_7^{(2),p} &= C_F^2\,\Big(- \frac{22152157463880329586222821137 47}{37155821787587543040000 0} - \frac{16384}{5005}\,\zeta(2)\,\ln 2\\
&+ \frac{2048}{1001}\,\zeta(2) + \frac{1729993541168029561}{3487983206400}\,\zeta(3)\Big)\\
&+ C_F\,C_A\,\Big(- \frac{153383207574671098939909454 03}{87822851497934192640000 0} + \frac{8192}{5005}\,\zeta(2)\,\ln 2\\
&- \frac{8192}{15015}\,\zeta(2) + \frac{263558316028764511}{18137512673280}\,\zeta(3) + \frac{445310672}{430404975}\,\ln\frac{\mu^2}{m^2}\Big)\\
&+ C_F\,T\,n_l\,\Big(- \frac{64850722258864}{213263513087625} - \frac{8192}{15015}\,\zeta(2) - \frac{1781242688}{4734454725}\,\ln\frac{\mu^2}{m^2}\Big)\\
&+ C_F\,T\,\Big(- \frac{190892441981633663}{66655359074304000} + \frac{16384}{15015}\,\zeta(2)\\
&+ \frac{253247865}{268435456}\,\zeta(3) - \frac{1781242688}{4734454725}\,\ln\frac{\mu^2}{m^2}\Big),\\
C_8^{(2),p} &= C_F^2\,\Big(- \frac{10182525636301604403651577979760 11}{33367107515151632302080000 0} - \frac{114688}{36465}\,\zeta(2)\,\ln 2\\
&+ \frac{14336}{7293}\,\zeta(2) + \frac{2147053611303928741345 87}{84572630522265600}\,\zeta(3)\Big)\\
&+ C_F\,C_A\,\Big(- \frac{23664024666626948756820830643 73}{33429013094957108428800000}\,\zeta(2) + \frac{57344}{36465}\,\zeta(2)\,\ln 2\\
&- \frac{57344}{109395}\,\zeta(2) + \frac{1106800878920761371869}{18793917893836800}\,\zeta(3) + \frac{78196015136}{84666807225}\,\ln\frac{\mu^2}{m^2}\Big)\\
&+ C_F\,T\,n_l\,\Big(- \frac{10872485544378464}{41951979645951375} - \frac{57344}{109395}\,\zeta(2) - \frac{312784060544}{931334879475}\,\ln\frac{\mu^2}{m^2}\Big)\\
&+ C_F\,T\,\Big(- \frac{4465014818406761701847}{1468550871125065728000} + \frac{114688}{109395}\,\zeta(2)\\
&+ \frac{132010901659}{115964116992}\,\zeta(3) - \frac{312784060544}{931334879475}\,\ln\frac{\mu^2}{m^2}\Big) \qquad \text{(C.4)}
\end{aligned}
$$

For the vector case the first seven moments were already presented in [6]. All other results are new.

References

[1] K.G. Chetyrkin, J.H. Kühn and A. Kwiatkowski, *Phys. Rept.* **277** (1996) 189.

[2] S.G. Gorishny, A.L. Kataev and S.A. Larin, *Phys. Lett.* **B 259** (1991) 144;
L.R. Surguladze and M.A. Samuel, *Phys. Rev. Lett.* **66** (1991) 560; (E) ibid., 2416;
K.G. Chetyrkin, *Phys. Lett.* **B 391** (1997) 402.

[3] K.G. Chetyrkin, *Phys. Lett.* **B 390** (1997) 309.

[4] K.G. Chetyrkin, R. Harlander, J.H. Kühn and M. Steinhauser, MPI/PhT/97-012, TTP97-11, hep-ph/9704222.

[5] R. Harlander and M. Steinhauser, MPI/PhT/97-013, TTP97-12, hep-ph/9704436.

[6] K.G. Chetyrkin, J.H. Kühn and M. Steinhauser, *Phys. Lett.* **B 371** (1996) 93; *Nucl. Phys.* **B 482** (1996) 213.

[7] F.V. Tkachov, *Phys. Lett.* **B 100** (1981) 65;
K.G. Chetyrkin and F.V. Tkachov, *Nucl. Phys.* **B 192** (1981) 159.

[8] S.G. Gorishny, A.L. Kataev and S.A. Larin *Nuovo Cim.* **92A** (1986) 119;
S.G. Gorishny, A.L. Kataev and S.A. Larin and L.R. Surguladze, *Mod. Phys. Lett.* **A 5** (1990) 2703;
K.G. Chetyrkin and A. Kwiatkowski, *Z. Phys.* **C 59** (1993) 525;
L.R. Surguladze, *Phys. Lett.* **B 338** (1994) 229;
L.R. Surguladze, *Phys. Lett.* **B 341** (1994) 60;
K.G. Chetyrkin, C.A. Dominguez, D. Pirjol and K. Schilcher; *Phys. Rev.* **D 51** (1995) 5090;
K.G. Chetyrkin and A. Kwiatkowski, *Nucl. Phys.* **B 461** (1996) 3;
L.R. Surguladze, *Phys. Rev.* **D 54** (1996) 2118;
K.G. Chetyrkin and J.H. Kühn, MPI/PhT/96-084, hep-ph/9609202.

[9] J.A.M. Vermaseren, *Symbolic Manipulation with FORM*, (Computer Algebra Netherlands, Amsterdam, 1991).

[10] D.J. Broadhurst, *Z. Phys.* **C 54** (1992) 54.

[11] J. Jersák, E. Laermann and P. Zerwas, *Phys. Rev.* **D 25** (1982) 1218;
L.J. Reinders, H. Rubinstein and S. Yazaki, *Nucl. Phys.* **B 186** (1981) 109.

[12] M. Drees and K. Hikasa, *Phys. Lett.* **B 240** (1990) 455; (E) ibid. **B 262** (1991) 497.

[13] A.H. Hoang, J.H. Kühn and T. Teubner, *Nucl. Phys.* **B 452** (1995) 173.

[14] L.D. Landau and E.M. Lifschitz, *Lehrbuch der Theoretischen Physik III, Quantenmechanik*, §36, Eq. (24);
A. Messiah, *Quantenmechanik 1*, Eq. (B32/2);
V.S. Fadin and V.A. Khoze, *Yad. Fiz.* **53** (1991) 1118.

[15] A.H. Hoang and T. Teubner, *private communication.*

[16] K. Melnikov, *Phys. Rev.* **D 53** (1996) 5020.

[17] K.G. Chetyrkin, A.H. Hoang, J.H. Kühn, M. Steinhauser and T. Teubner, *Phys. Lett.* **B 384** (1996) 233.

[18] P.A. Baikov and D.J. Broadhurst, presented at the *4th International Workshop on Software Engineering and Artificial Intelligence for High Energy and Nuclear Physics (AIHENP95), Pisa, Italy, 3-8 April 1995.* Published in Pisa AIHENP (1995) 167.

[19] G. Källén and A. Sabry, *K. Dan. Vidensk. Selsk. Mat.-Fys. Medd.* **29** (1955) No. 17;
R. Barbieri and E. Remiddi, *Nuovo Cim.* **13A** (1973) 99;
B.A. Kniehl, *Nucl. Phys.* **B 347** (1990) 65;
D.J. Broadhurst, J. Fleischer and O.V. Tarasov, *Z. Phys.* **C 60** (1993) 287.

[20] A. Djouadi and P. Gambino, *Phys. Rev.* **D 51** (1995) 218; (E) ibid. **D 53** (1996) 4111;
see also: D.J. Broadhurst, *Phys. Lett.* **B 101** (1981) 423.

[21] K.G. Chetyrkin and J.H. Kühn, *Nucl. Phys.* **B 432** (1994) 337.

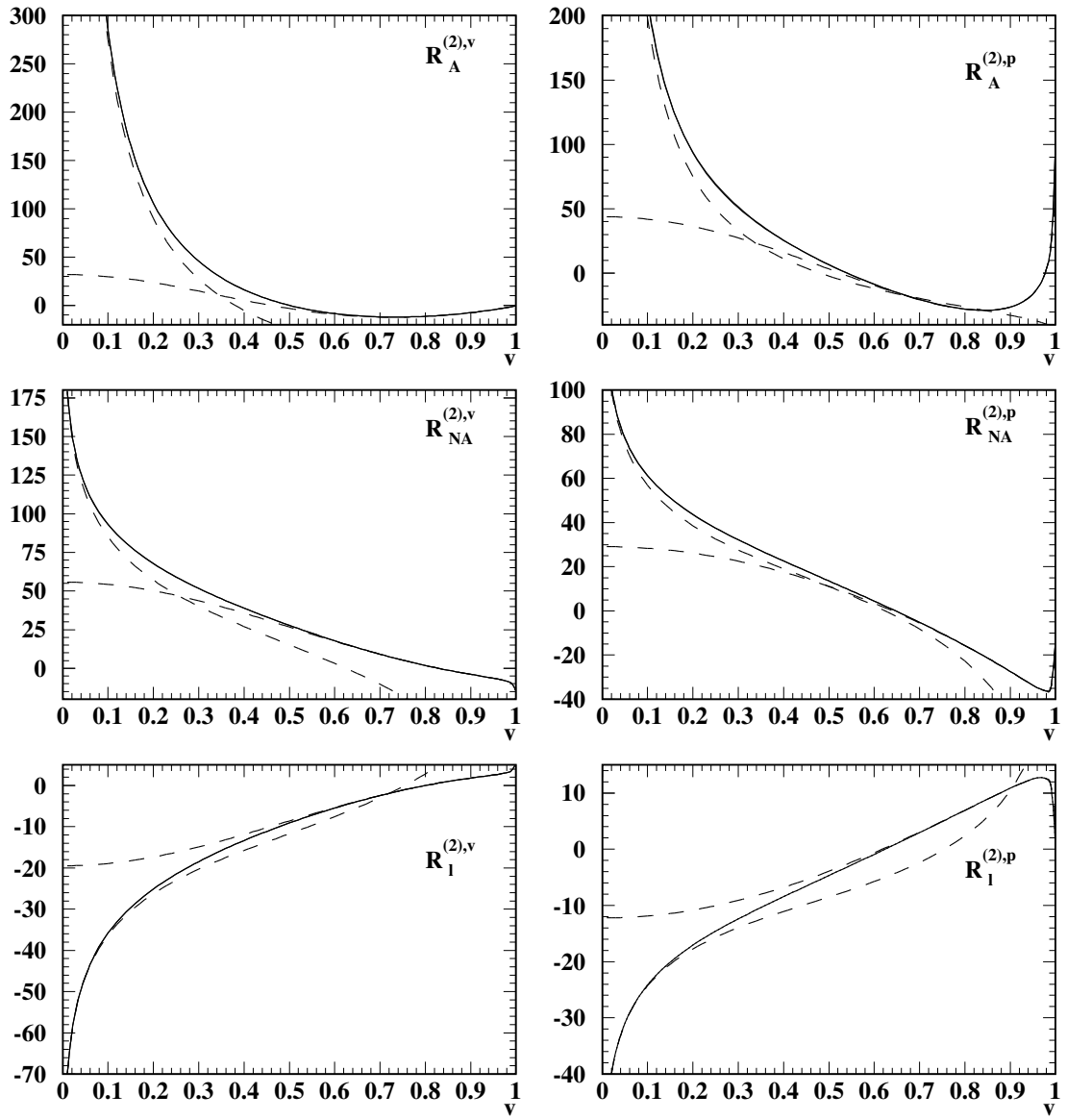

Figure 1: $R^{(2),v}$ and $R^{(2),p}$ plotted against v. The dashed curves represent the threshold and the high energy approximations, respectively. Whereas for the vector case also the terms of order $(m^2/s)^6$ are available [4] for the pseudo-scalar correlator terms of order $(m^2/s)^4$ [5] are plotted.

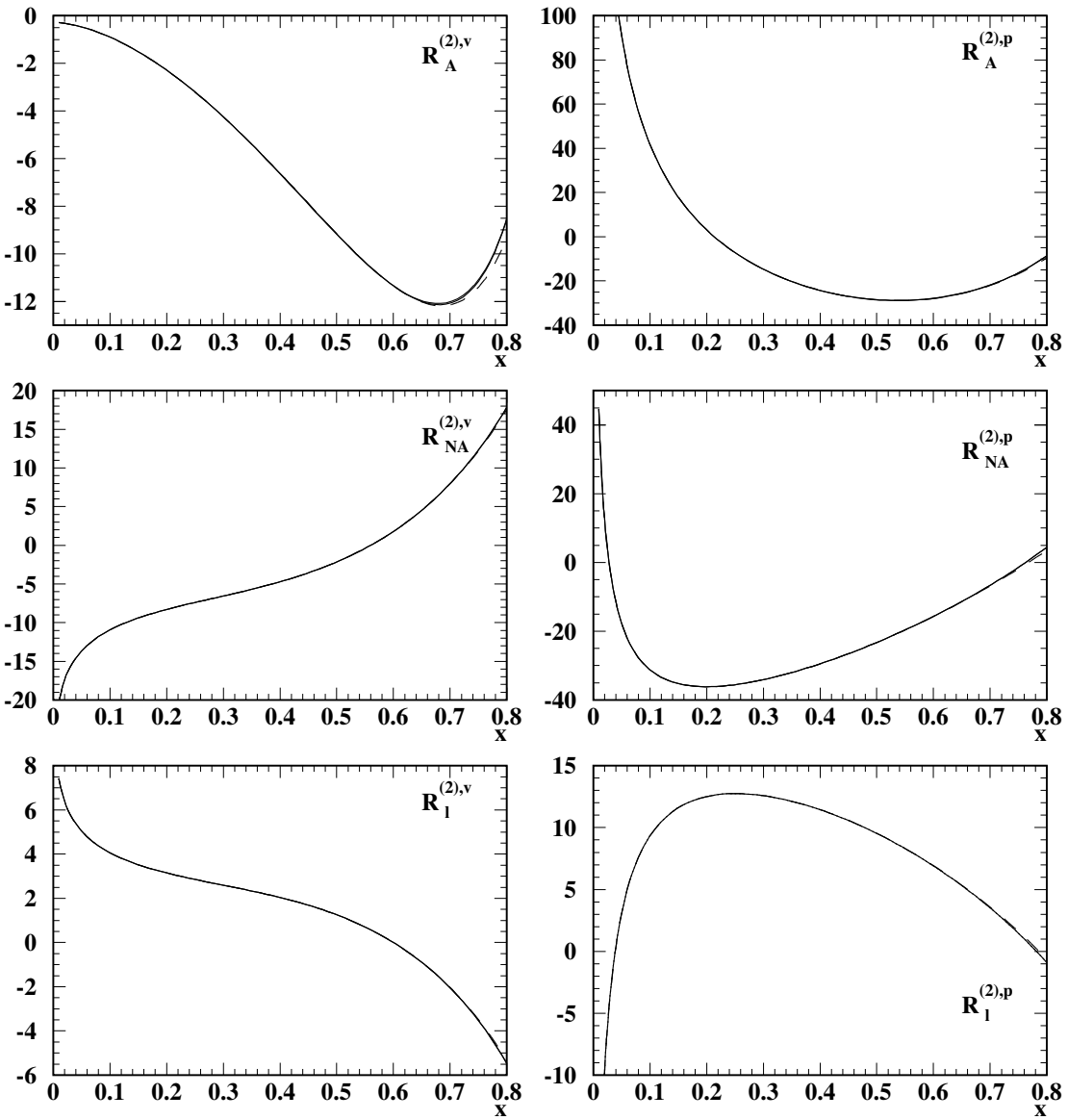

Figure 2: $R^{(2),v}$ and $R^{(2),p}$ plotted against x. The dashed curves represent the high energy approximations including terms up to $\mathcal{O}(x^{12})$ for the vector correlator and $\mathcal{O}(x^8)$ for the pseudo-scalar case.

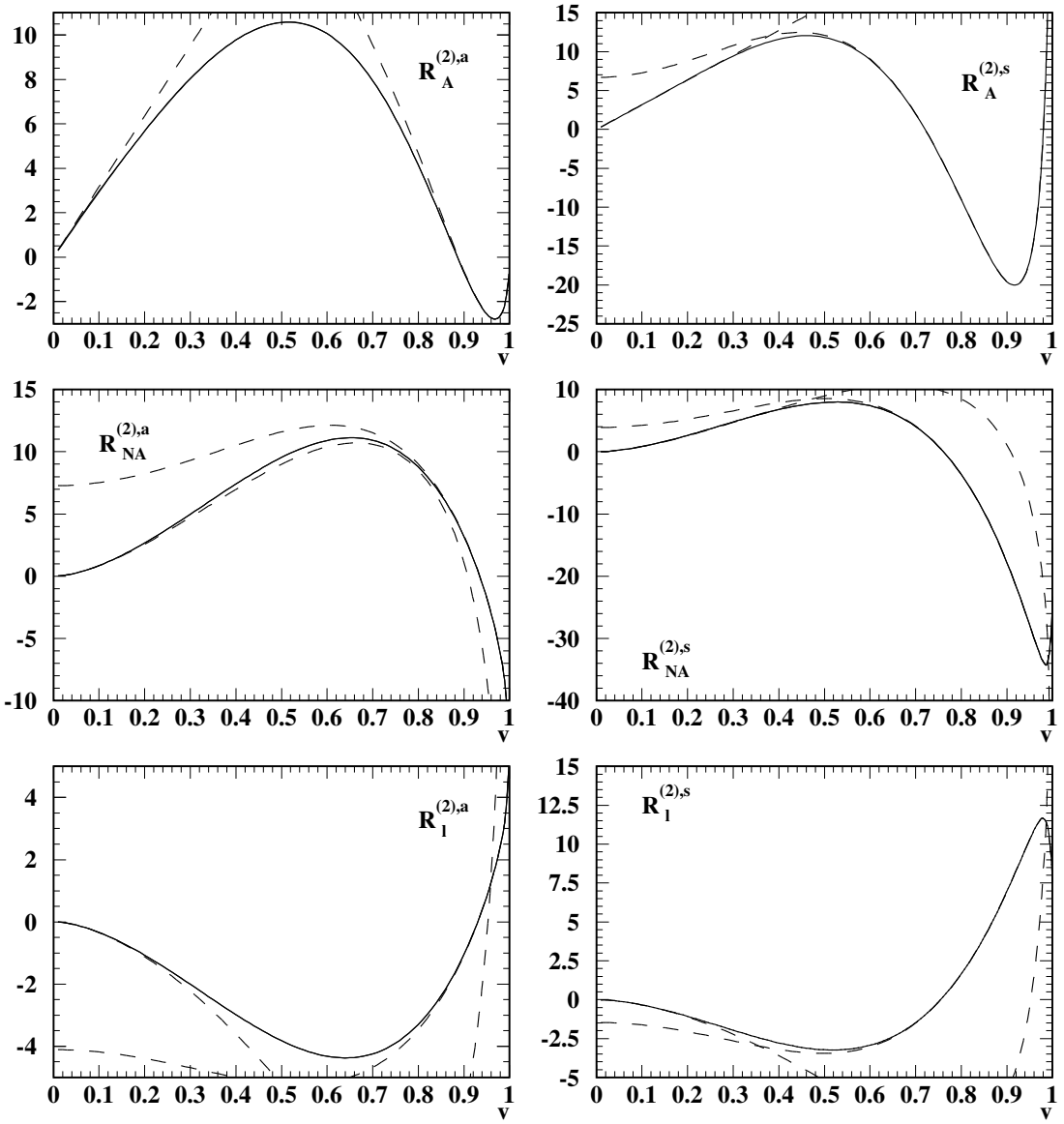

Figure 3: $R^{(2),a}$ and $R^{(2),s}$ plotted against v. The dashed curves represent the threshold and the high energy approximations, respectively. For the axial-vector case terms of order $(m^2/s)^4$ are available [21] and for the scalar correlator terms of order $(m^2/s)^4$ [5] are plotted.

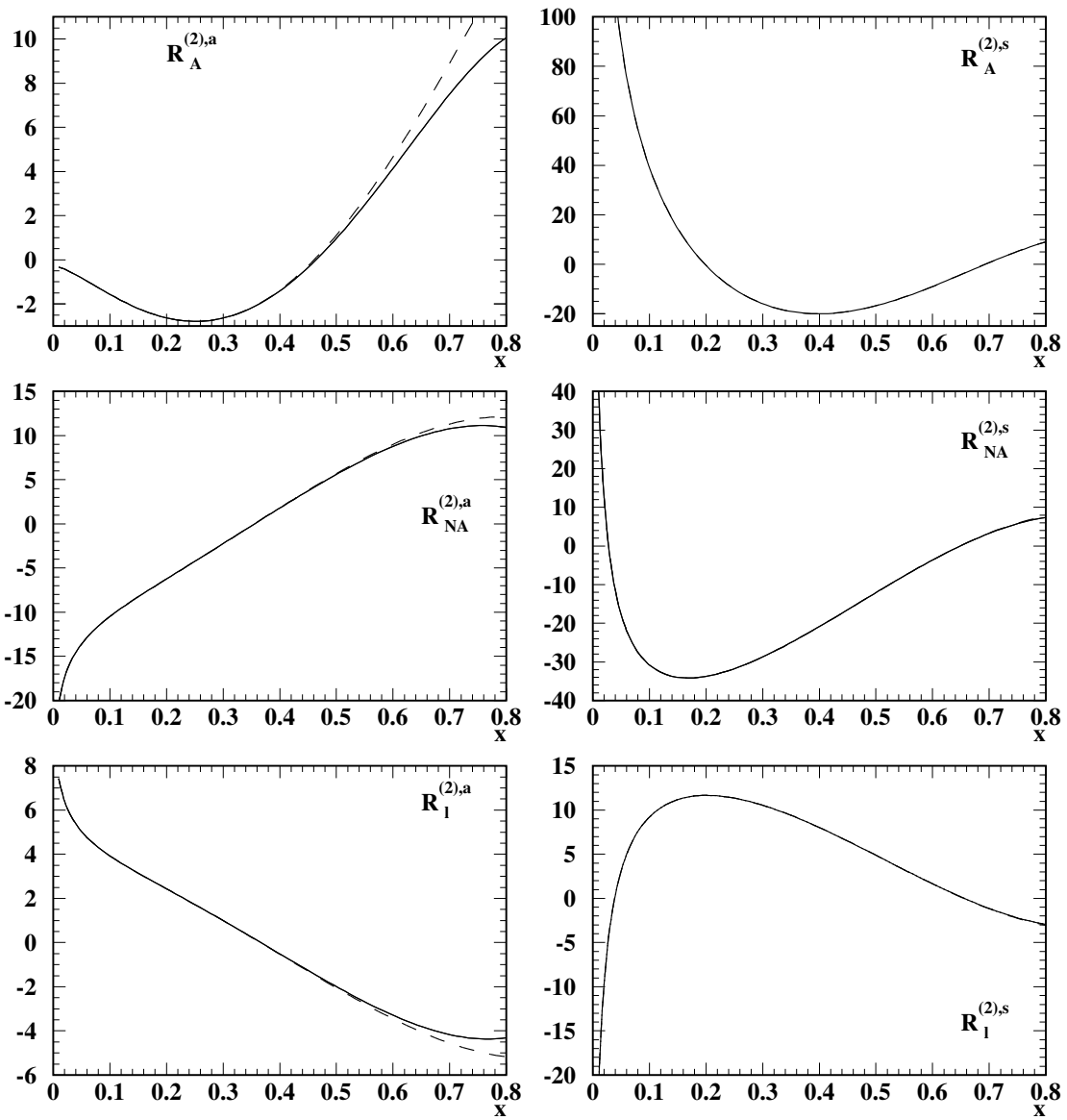

Figure 4: $R^{(2),a}$ and $R^{(2),s}$ plotted against x. The dashed curves represent the high energy approximations including terms up to $\mathcal{O}(x^4)$ for the axial-vector correlator and $\mathcal{O}(x^8)$ for the scalar case.

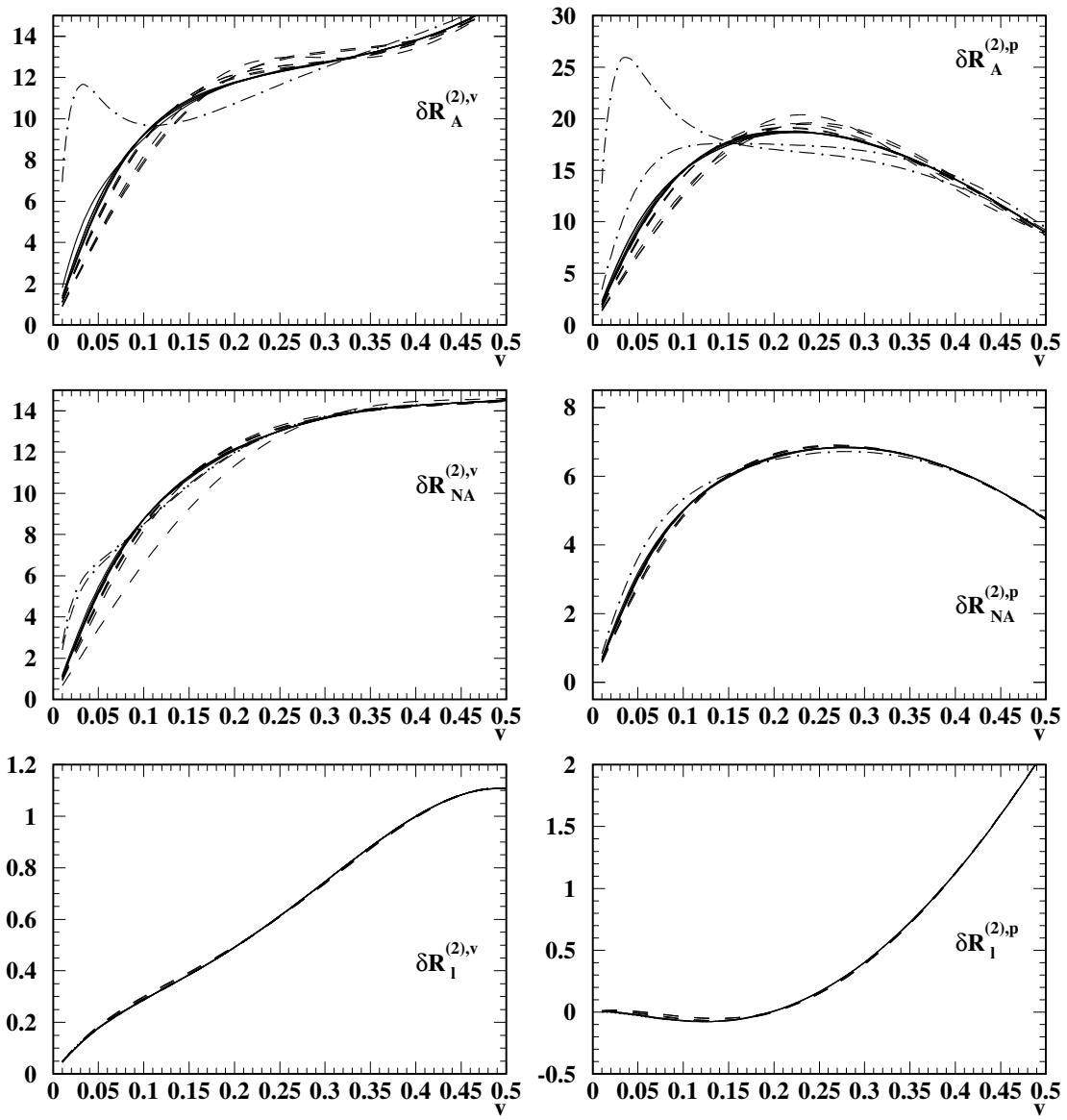

Figure 5: $R^{(2),v}$ and $R^{(2),p}$ plotted against v. The leading threshold terms are subtracted. The dashed lines contain only information up to C_6 whereas for the full curves also C_7 and C_8 is used. The obvious exceptions are represented by the dash-dotted curves. They are described in the text.

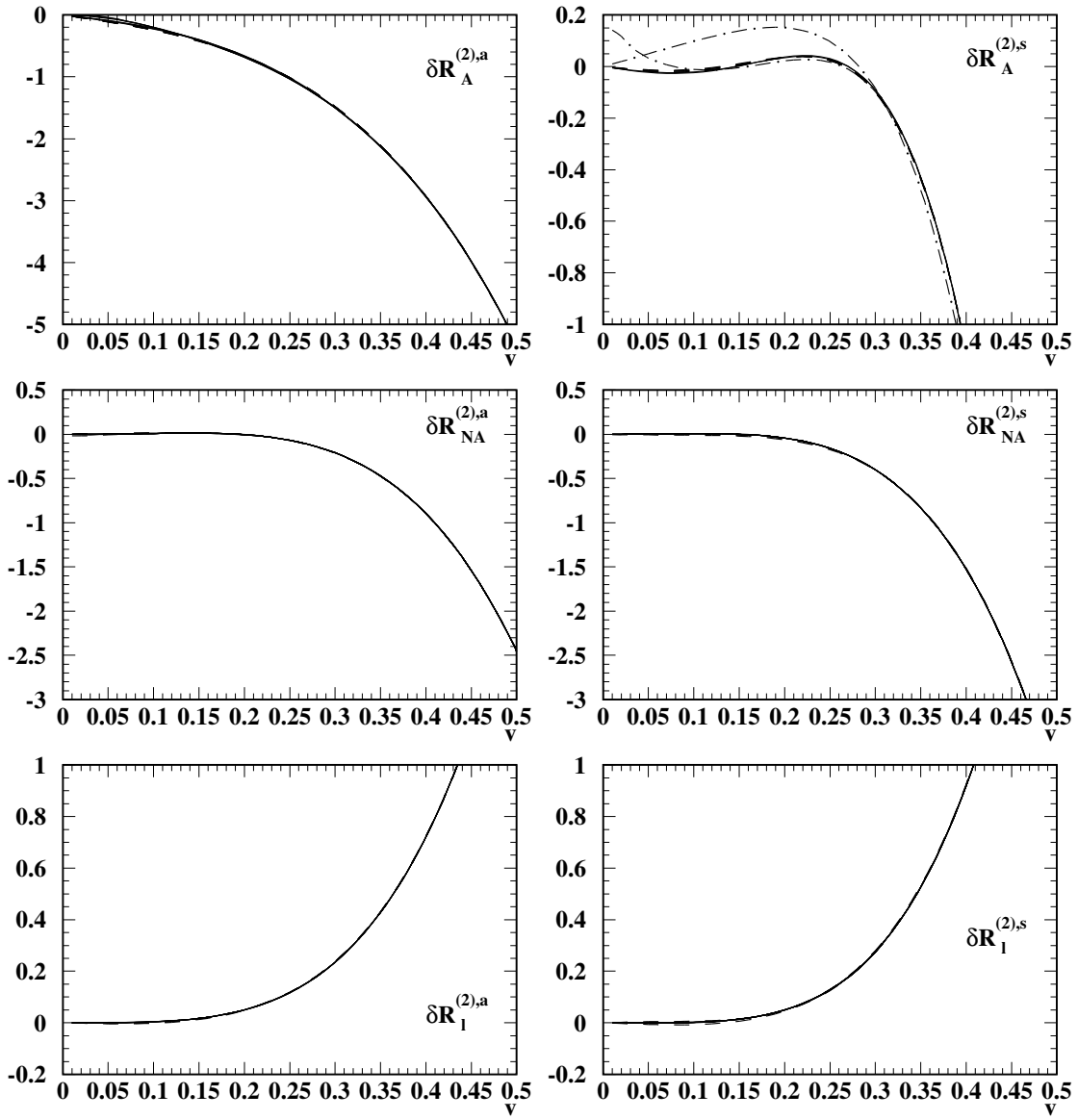

Figure 6: $R^{(2),a}$ and $R^{(2),s}$ plotted against v. The leading threshold terms are subtracted. The same notation as in Fig. 5 is adopted.

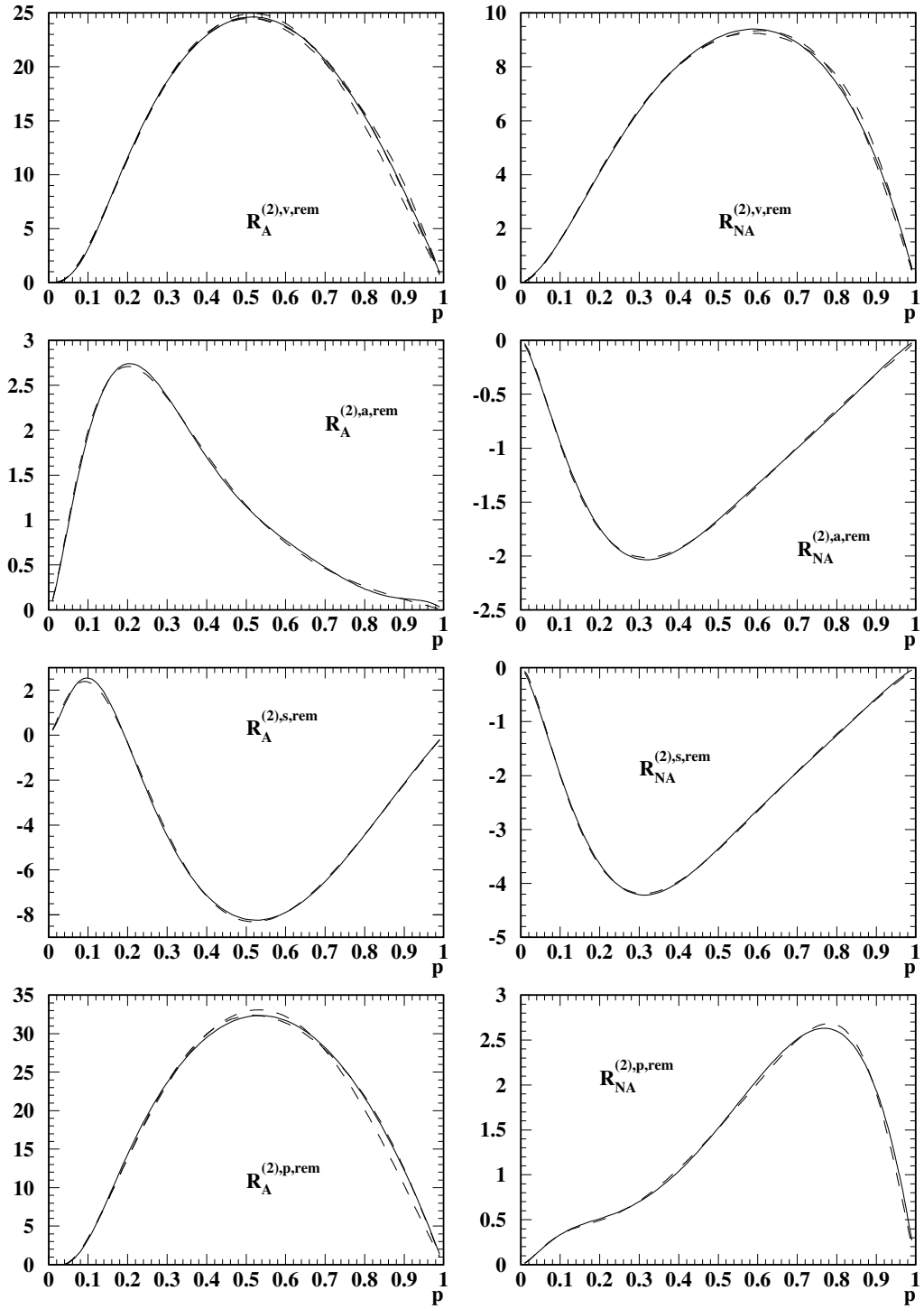

Figure 7: The remainder $R_x^{(2),\delta,rem}$, $x \in \{A, NA\}$ is plotted for different Padé approximants (dashed lines) together with the fit (solid line).